sitagliptin and glimepiride groups compared with that by 0.03 kg in the glimepiride alone group (6). However, the average dose of SUs was higher (2.46 mg) compared with that in our study (1.19 mg). The decrease in dosage of SUs might thus be a cause of the BMI reduction in glimepiride subjects.

Blood pressure and urinary albumin excretion in 52-week also were significantly decreased compared with those at baseline without any change of other medications including statin and angiotensin receptor blocker. Systolic and diastolic blood pressures were decreased by 6.7 mmHg (95% CI −10.0 to −3.4) and 3.6 mmHg (95% CI −4.8 to −3.4) respectively. Urinary albumin excretion was reduced by 43.2 mg/gCr (95% CI −65.7 to −20.8). Ogawa et al. reported that systolic blood pressure was dropped from 130.0 ± 37.2 to 119.7 ± 9.4 mmHg by the treatment of sitagliptin in Japanese hypertensive patients with type 2 diabetes (21). Another study reported that systolic blood pressure was decreased from 133.0 ± 0.9 to 130.0 ± 0.7 mmHg, and diastolic blood pressure from 75.2 ± 0.7 to 73.4 ± 0.7 mmHg (19). Hattori reported that urinary albumin excretion was decreased from 11.6 ± 8.4 to 4.5 ± 5.0 mg/gCr in 6-month (22). GLP-1 enhances sodium excretion and reduces hyperfiltration in obese men (23). Liraglutide, a GLP-1 receptor agonist, decreased systolic blood pressure (24,25). Exenatide, another GLP-1 receptor agonist, also reduced systolic blood pressure (26). For these reasons, the increased active GLP-1 level by sitagliptin might have decreased the blood pressure level and urinary albumin excretion in our study.

Insulin secretion capacity evaluated by glucagon loading test at 52-week was not significantly changed compared with that at baseline. However, all AHAs including sitagliptin were unmedicated for 72 h before the glucagon loading test at 52-week. Under this condition, 0-min C-peptide, 6-min C-peptide, CPI and SUIT index at 52-week were almost the same as those at baseline. These results indicate that insulin secretion capacity was preserved at least for 1 year by the treatment with SUs and sitagliptin. For vildaglipitin, another DPP-4 inhibitor, it has been reported that beta-cell function was preserved by 2-year treatment under condition of 4-week washout (12). Sitagliptin also may improve beta cell function with longer term usage. Therefore, a glucagon loading test is scheduled 2 years after the initiation of combination therapy with sitagliptin and low dosage of SUs.

In summary, combination therapy with sitagliptin and low dosage of SUs is effective for glycaemic control in Japanese type 2 diabetes. The combination therapy is weight neutral, and lowered both the blood pressure level and urinary albumin excretion. As a result of this decrease in the dosage of SUs, hypoglycaemia seldom occurs, and there is no severe hypoglycaemia. When sitagliptin is added on to SUs for the first time, the initial dosage of glimepiride or gliclazide should be less than 2 mg/day and 40 mg/day, respectively, according to the committee's recommendation regarding use of incretin-based therapy.

Author contributions

The study conception and protocol were by Shin-ichi Harashima and Nobuya Inagaki. Patient examinations were by Shin-ichi Harashima, Toru Fukushima, Tadashi Koizumi and Mitsuru Aono. Collection of data was by Yu Wang, Yuko Murata and Mika Seike. The statistical analysis was by Daisuke Tanaka, Shunsuke Yamane and Masahito Ogura. The manuscript development was by Shin-ichi Harashima and Nobuya Inagaki. All authors reviewed and approved the final version of the manuscript.

References

1 Nathan DM, Buse JB, Davidson MB et al. American Diabetes Association; European Association for Study of Diabetes. Medical management of hyperglycemia in type 2 diabetes: a consensus algorithm for the initiation and adjustment of therapy: a consensus statement of the American Diabetes Association and the European Association for the Study of Diabetes. *Diabetes Care* 2009; **32**: 193–203.

2 Arai K, Matoba K, Hirao K et al. Present status of sulfonylurea treatment for type 2 diabetes in Japan: second report of a cross-sectional survey of 15,652 patients. *Endocr J* 2010; **57**: 499–507.

3 Tahrani AA, Bailey CJ, Del Prato S, Barnett AH. Management of type 2 diabetes: new and future developments in treatment. *Lancet* 2011; **378**: 182–97.

4 Nonaka J, Kakikawa T, Sato A et al. Efficacy and safety of sitagliptin monotherapy in Japanese patients with type 2 diabetes. *Diabetes Res Clin Pract* 2008; **79**: 291–8.

5 Tajima N, Kadowaki T, Odawara M, Nishi M, Taniguchi T, Arjona Ferreira JC. Addition of sitagliptin to ongoing glimepiride therapy in Japanese patients with type 2 diabetes over 52 weeks leads to improved glycemic control. *Diabetol Int* 2011; **2**: 32–44.

6 Hermansen K, Kipnes M, Luo E, Fanurik D, Khatami H, Stein P. Efficacy and safety of the dipeptidyl peptidase-4 inhibitor, sitagliptin, in patients with type 2 diabetes mellitus inadequately controlled on glimepiride alone or on glimepiride and metformin. *Diabetes Obes Metab* 2007; **9**: 733–45.

7 Vilsbøll T, Rosenstock J, Yki-Järvinen H et al. Efficacy and safety of sitagliptin when added to insulin therapy in patients with type 2 diabetes. *Diabetes Obes Metab* 2010; **12**: 167–77.

8 Iwakura T, Fujimoto K, Tahara Y, Matsuoka N, Ishihara T, Seino Y. A case of severe hypoglycemia induced by sitagliptin added to ongoing glimepiride therapy in patients with type 2 diabetes. *J Jpn Diabetes Soc* 2010; **53**: 505–8.

9 Sitagliptin post-marketing surveillance study (in Japanese). MSD KK. August 2010.

10 Inagaki N, Iwakura T, Iwamoto Y, Kadowaki T, Seino S, Seino Y. *The committee regarding to adequate use for incretin-based therapy*. http://www.nitto-kyo.or.jp/kinkyu_incretin100408m.html

11 Holman RR. Long-term efficacy of sulfonylureas: a United Kingdom prospective diabetes study perspective. *Metabolosm* 2006; **55**: S2–5.

12 Scherbaum WA, Schweizer A, Mari A et al. Evidence that vildagliptin attenuates deterioration of glycaemic control during 2-year treatment of patients with type 2 diabetes and mild hyperglycaemia. *Diabetes Obes Metab* 2008; **10**: 1114–24.

13 The Committee of Japan Diabetes Society on the diagnostic criteria of diabetes mellitus. Report of

the Committee on the classification and diagnostic criteria of diabetes mellitus. *J. Jpn. Diabetes Soc* 2010; **53**: 450–67.
14 Funakoshi S, Fujimoto S, Hamasaki A et al. Analysis of factors influencing pancrfeatic beta^cell function in Japanese patients with type 2 diabetes: association with body mass index and duration of diabetic exposure. *Diabetes Res Clin Pract* 2008; **82**: 353–8.
15 Yamada Y, Fukuda K, Fujimoto S et al. SUIT, secretory units of islets in transplantation: an index for therapeutic management of islet transplanted patients and its application to type 2 diabetes. *Diabetes Res Clin Pract* 2006; **74**: 222–6.
16 Ahren Bo. Use of DPP-4 inhibitors in type 2 diabetes: focus on sitagliptin. *Diabetes Metab Syndr Obes* 2010; **3**: 31–41.
17 Williams-Herman D, Engel SS, Round E et al. Safety and tolerability of sitagliptin in clinical studies: a pooled analysis of data from 10,246 patients with type 2 diabetes. *BMC Endocr Disord* 2010; **10**: 7–28.
18 Hurren KM, Bartley EP, O'Neill JL, Ronis DL. Effect of sulfonylurea dose escalation on hemoglobin A1c in Veterans Affairs patients with type 2 diabetes. *Acta Diabetol* 2010. doi: 10.1007/s00592-010-0197-1.
19 Kim SA, Shim WH, Lee EH et al. Predictive clinical parameters for the therapeutic efficacy of sitagliptin in Korean type 2 diabetes mellitus. *Diabetes Metab J* 2011; **35**: 159–65.
20 Nomiyama T, Akei Y, Takenoshita H, nagashi R, Terawaki Y, Nagasako H. Contributing factors related to efficacy of the dipeptidyl peptidase-4 inhibitor sitagliptin in Japanese patients with type 2 diabetes. *Diabetes Res Clin Pract* 2012; **95**: e27–28.
21 Ogawa S, Ishiki M, Nako K et al. Sitagliptin, a dipeptidyl peptidase-4 inhibitor, decreases systolic blood pressure in Japanese hypertensive patients with type 2 diabetes. *Tohoku J Exp Med* 2011; **223**: 133–5.
22 Hattori S. Sitagliptin reduces albuminuria in patients with type 2 diabetes. *Endocr J* 2011; **58**: 69–73.
23 Gutzwiller JP, Tschopp S, Bock A et al. Glucagon-like peptide 1 induces natriuresis in healthy subjects in insulin-resistant obese men. *J Clin Endocrinol Metab* 2004; **89**: 3055–61.
24 Yang W, Chen L, Ji Q et al. Liraglutide provides similar glycemic control as glimepiride (both in combination with metformin) and reduces body weight and systolic blood pressure in Asian population with type 2 diabetes from China, South Korea and India: a 16-week, randomized, double-blind, active control trial. *Diabetes Obes Metab* 2011; **13**: 81–8.
25 Garber A, Henry R, Ratner R et al. LEAD-3 (Mono) Study Group. Liraglutide versus glimepiride monotherapy for type 2 diabetes (LEAD-3 Mono): a randomised, 52-week, phase III, double-blind, parallel-treatment trial.Zdravkovic M, Bode B; LEAD-3 (Mono) Study Group. *Lancet* 2009; **373**: 473–81.
26 Gill A, Hoogwerf BJ, Burger J et al. Effect of exenatide on heart rate and blood pressure in subjects with type 2 diabetes mellitus: a double-blind, placebo-controlled, randomized pilot study. *Cardiovasc Diabetol* 2010; **9**: 6–13.

Paper received November 2011, accepted January 2012

Exendin-4 Suppresses Src Activation and Reactive Oxygen Species Production in Diabetic Goto-Kakizaki Rat Islets in an Epac-Dependent Manner

Eri Mukai,[1,2] Shimpei Fujimoto,[1] Hiroki Sato,[1] Chitose Oneyama,[3] Rieko Kominato,[1] Yuichi Sato,[1] Mayumi Sasaki,[1] Yuichi Nishi,[1] Masato Okada,[3] and Nobuya Inagaki[1,4]

OBJECTIVE—Reactive oxygen species (ROS) is one of most important factors in impaired metabolism secretion coupling in pancreatic β-cells. We recently reported that elevated ROS production and impaired ATP production at high glucose in diabetic Goto-Kakizaki (GK) rat islets are effectively ameliorated by Src inhibition, suggesting that Src activity is upregulated. In the present study, we investigated whether the glucagon-like peptide-1 signal regulates Src activity and ameliorates endogenous ROS production and ATP production in GK islets using exendin-4.

RESEARCH DESIGN AND METHODS—Isolated islets from GK and control Wistar rats were used for immunoblotting analyses and measurements of ROS production and ATP content. Src activity was examined by immunoprecipitation of islet lysates followed by immunoblotting. ROS production was measured with a fluorescent probe using dispersed islet cells.

RESULTS—Exendin-4 significantly decreased phosphorylation of Src Tyr416, which indicates Src activation, in GK islets under 16.7 mmol/l glucose exposure. Glucose-induced ROS production (16.7 mmol/l) in GK islet cells was significantly decreased by coexposure of exendin-4 as well as PP2, a Src inhibitor. The Src kinase–negative mutant expression in GK islets significantly decreased ROS production induced by high glucose. Exendin-4, as well as PP2, significantly increased impaired ATP elevation by high glucose in GK islets. The decrease in ROS production by exendin-4 was not affected by H-89, a PKA inhibitor, and an Epac-specific cAMP analog (8CPT-2Me-cAMP) significantly decreased Src Tyr416 phosphorylation and ROS production.

CONCLUSIONS—Exendin-4 decreases endogenous ROS production and increases ATP production in diabetic GK rat islets through suppression of Src activation, dependently on Epac. ***Diabetes* 60:218–226, 2011**

From the [1]Department of Diabetes and Clinical Nutrition, Graduate School of Medicine, Kyoto, University, Kyoto, Japan; the [2]Japan Association for the Advancement of Medical Equipment, Tokyo, Japan, the [3]Department of Oncogene Research, Research Institute for Microbial Diseases, Osaka University, Osaka, Japan; and the [4]Core Research for Evolutional Science and Technology of Japan Science and Technology Cooperation, Kyoto, Japan.

Corresponding author: Shimpei Fujimoto, fujimoto@metab.kuhp.kyoto-u.ac.jp.

Received 6 January 2010 and accepted 12 October 2010. Published ahead of print at http://diabetes.diabetesjournals.org on 26 October 2010. DOI: 10.2337/db10-0021.

In pancreatic β-cells, glucose metabolism regulates exocytosis of insulin granules through metabolism secretion coupling, in which glucose-induced ATP production in mitochondria plays an essential role (1). Impairment of mitochondrial ATP production causes reduced glucose-induced insulin secretion.

Reactive oxygen species (ROS) is one of the most important factors that impair metabolism secretion coupling in β-cells. Exposure to exogenous hydrogen peroxide (H_2O_2), the most abundant ROS, reduces glucose-induced insulin secretion by impairing mitochondrial metabolism in β-cells (2,3). However, little is known of the role of endogenous ROS in impaired glucose-induced insulin secretion from β-cells. Some studies (4,5) have shown that endogenous ROS is produced in mitochondria by exposure to high glucose. In Zucker diabetic fatty rats, the superoxide content of islets at basal glucose levels is higher than that in Zucker lean control rats (4). Furthermore, we recently reported that high glucose–induced ROS production in islet cells is elevated in diabetic Goto-Kakizaki (GK) rats compared with control Wistar rats (6). Thus, endogenous ROS production is elevated in β-cells under diabetic pathophysiological conditions.

Although the mechanism of endogenous ROS production in β-cells in the diabetic state remains largely unknown, we have reported that Src (c-Src) plays an important role in the signal transduction that produces ROS (6). Src is a nonreceptor tyrosine kinase that is associated with the cell membrane and plays important roles in various signal transductions, and its activity is regulated by intramolecular interactions that depend on tyrosine phosphorylation (7,8). Phosphorylation of Tyr527 (Tyr529 in humans), which is located near the C terminus of Src, is brought about by COOH terminal Src kinase (Csk), a negative regulator of Src (9), and holds the kinase in the inactive form. Dephosphorylation of Tyr527 followed by disruption of the intramolecular interaction allows phosphorylation of Tyr416 (Tyr418 in humans) at the kinase domain, resulting in Src activation. In our previous report (6), PP2, a selective Src inhibitor, decreased high-glucose–induced ROS production in GK islet cells, in contrast to the lack of any effect of the agent in Wistar islet cells, suggesting that Src may be activated in the diabetic condition and cause elevation of ROS production in the presence of high glucose.

Glucagon-like peptide (GLP)-1 is one of the incretin peptides released from the intestine in response to nutrient ingestion that augments glucose-induced insulin secretion from β-cells (10,11). GLP-1 binding to the GLP-1 receptor, a member of the G protein–coupled receptor

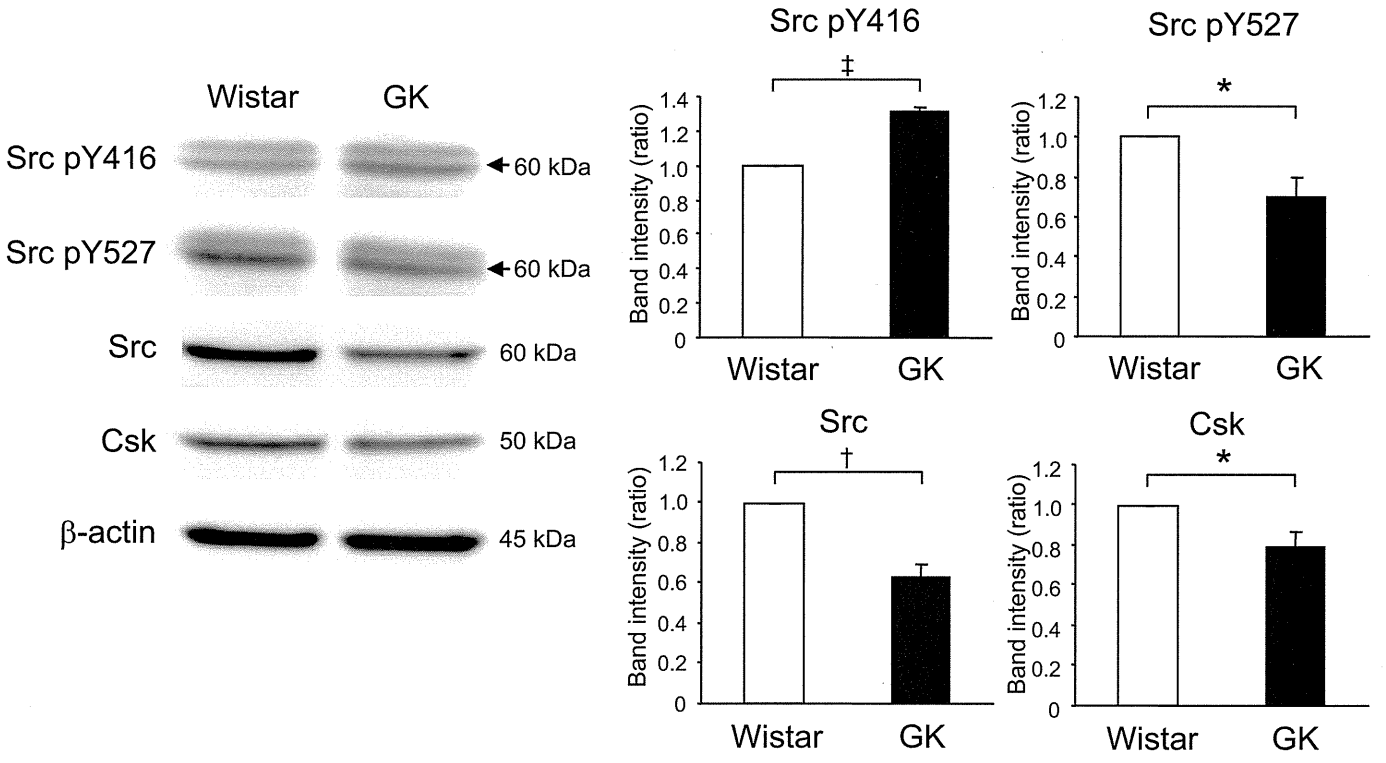

FIG. 1. Comparison of expression of Src between fresh Wistar and GK islets. Fresh islets were lysated and subjected to immunoblot analyses. Blots (50 μg of protein) were probed with anti–phospho-Src (Tyr^{416}), anti–phospho-Src (Tyr^{527}), anti-Src, or anti-Csk. The same blots were stripped and reprobed with anti–β-actin, respectively. Intensities of the bands were quantified with densitometric imager. The bar graphs are expressed relative to Wistar islet value corrected by β-actin level (means ± SE). *$P < 0.05$; †$P < 0.01$; ‡$P < 0.001$. Representative blot panels of three to five independent experiments are shown.

(GPCR) superfamily, induces activation of adenylyl cyclase and elevation of intracellular cAMP levels, which elicits protein kinase A (PKA)-dependent signal transduction. Recently, Epac (also known as cAMP-GEF [guanine nucleotide exchange factor]) has been shown to be a novel cAMP sensor in the PKA-independent pathway (12,13). In β-cells, one member of the Epac family, Epac2, has an important role in insulin secretion, especially in regulation of exocytosis of insulin granules (14,15). Previous studies have shown that GLP-1 also has beneficial long-term effects on diabetic β-cells, including induction of β-cell proliferation (16,17), enhanced resistance to apoptosis (17,18), and amelioration of endoplasmic reticulum stress (19). Furthermore, increased ROS in diabetic *db/db* mouse islets is decreased by treatment with an inhibitor of dipeptidyl peptidase IV that delays the degradation of GLP-1 (20).

In the present study, we investigated whether the GLP-1 signal directly ameliorates endogenous ROS production in diabetic GK islets using exendin-4, a GLP-1 receptor agonist. In particular, we focused on clarifying regulation of Src activity by GLP-1 signaling. We describe here both a novel effect and a mechanism of GLP-1 signaling that acutely decreases ROS production by high glucose through suppression of Src activation PKA independently and Epac dependently.

RESEARCH DESIGN AND METHODS

Male Wistar and GK rats were obtained from Shimizu (Kyoto, Japan). All experiments were carried out with rats that were aged ~7–8 weeks. Nonfasting blood glucose levels were ~160–240 mg/dl in the GK rats and ~70–120 mg/dl in the Wistar rats used in the experiments. The animals were maintained and used in accordance with the guidelines of the animal care committee of Kyoto University.

Islet preparation. Pancreatic islets were isolated from Wistar and GK rats by the collagenase digestion technique (6). Isolated islets were washed with Krebs Ringer bicarbonate buffer (KRBB) (in mmol/l: 129.4 NaCl, 5.2 KCl, 2.7 $CaCl_2$, 1.3 KH_2PO_4, 1.3 $MgSO_4$, and 24.8 $NaHCO_3$ [equilibrated with 5% CO_2/95% O_2, pH 7.4]) containing 2.8 mmol/l glucose and cultured for ~20 h in RPMI-1640 medium containing 5.5 mmol/l glucose and 10% FCS. Cultured islets were preincubated for 30 min at 37°C in KRBB supplemented with 0.2% BSA and 10 mmol/l HEPES (KRBB medium) containing 2.8 mmol/l glucose and incubated for the indicated times at 37°C in KRBB medium containing 16.7 mmol/l glucose with or without test materials.

Retroviral-mediated gene transfer. Production of retroviral vectors with pCX4 was performed as previously described (21). Src kinase–negative mutant (K295M) was subcloned into pCX4pur (22). Gene transfer experiments of islets were carried out by an in vivo gene transduction method (23). Briefly, after rats were anesthetized and subjected to laparotomy, the hepatic artery with the portal vein and the splenic artery were ligated. The upper side of the celiac artery that branches from the abdominal aorta was clamped, and 100 μl of retroviral vector suspension was injected into the lower side of the clamped point of the artery. The pancreatic islets were then isolated and cultured for 48 h before the experiment. Gene expression using green fluorescent protein–expressing vector was effective in the inside of the islets, as previously reported (23).

Immunoprecipitation and immunoblotting. Fresh or incubated islets were lysed in ice-cold lysis buffer (10 mmol/l Tris [pH 7.2], 100 mmol/l NaCl, 1 mmol/l EDTA, 1% Nonidet P-40, and 0.5% sodium deoxycholate) containing protease inhibitor cocktail (Complete; Roche, Mannheim, Germany), phosphatase inhibitor cocktail (Calbiochem, Darmstadt, Germany), and 5 mmol/l sodium pyrophosphate. For determination of Src activation, lysates were centrifuged at 560,000*g* for 10 min at 4°C, and the supernatant (~2 mg of protein content/2,500 islets) was mixed with 4 μg mouse monoclonal anti-Src antibody (clone GD11; Upstate, Billerica, MA) and 30 μl washed protein G Sepharose (GE Healthcare, Uppsala, Sweden) followed by gentle rotation for 4 h at 4°C. Immunoprecipitates or islet lysates (50 μg) were subjected to immunoblotting as previously described (23). Primary antibodies used were rabbit anti–phospho-Src (Tyr416) and anti–phospho-Src (Tyr527) from Biosource (Camarillo, CA); rabbit anti-Src, anti-Csk, anti-Epac2, extracellular signal–regulated kinase (ERK) 1/2, and mouse anti–phospho-ERK1/2 (Thr202/Tyr204) from Santa Cruz Biotechnology (Santa Cruz, CA); rabbit anti-Rap1 from Upstate; rabbit anti–phospho-Akt (Ser473) and anti-Akt from Cell

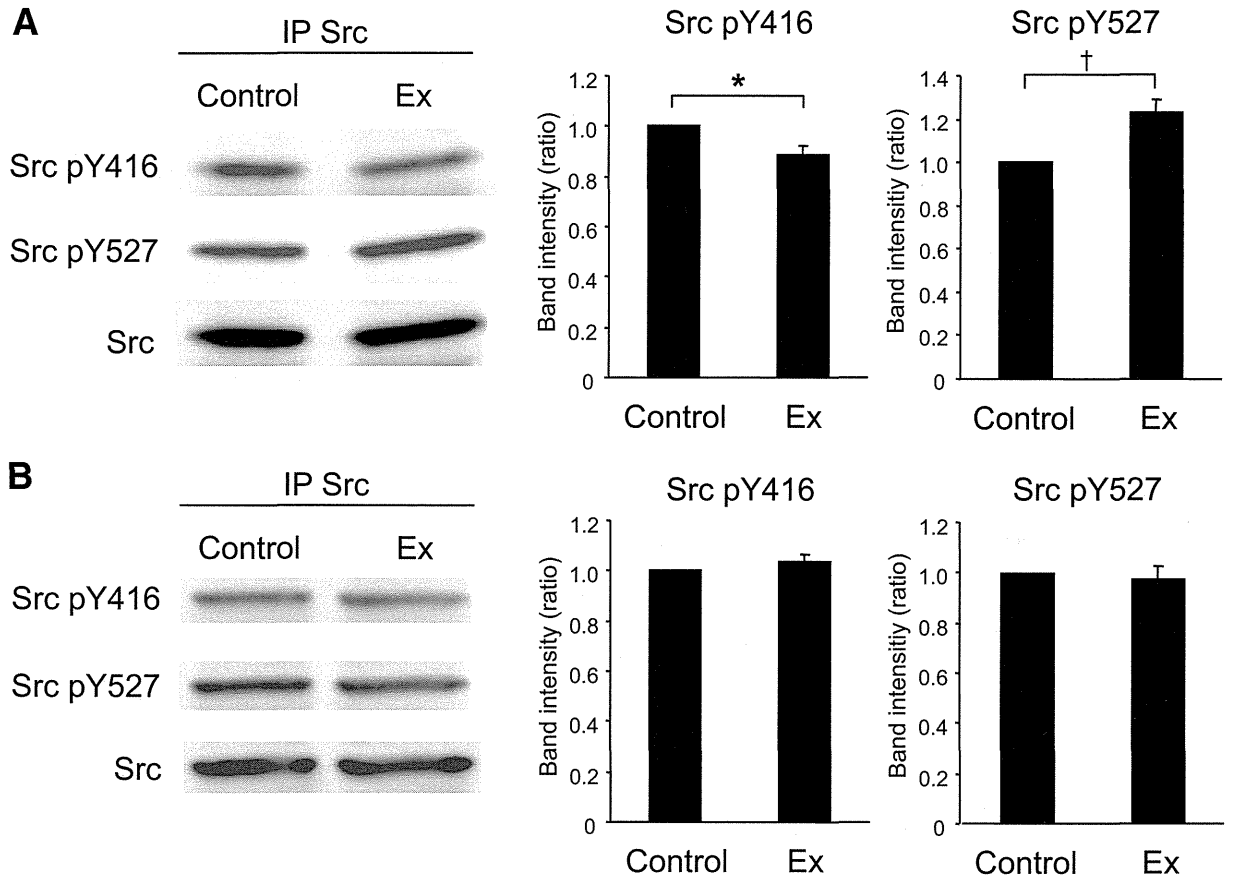

FIG. 2. Exendin-4 suppresses Src activity at high glucose in GK islets. Effects of exendin-4 on Src activity at high glucose in GK (*A*) and Wistar (*B*) islets. After preincubation in the presence of 2.8 mmol/l glucose for 30 min, islets were incubated in the presence of 16.7 mmol/l glucose with or without 100 nmol/l exendin-4 for 10 min. Islet lysates (~2 mg of protein) were immunoprecipitated with anti-Src antibody and subjected to immunoblot analyses. Blots were probed with anti–phospho-Src (Tyr^{416}), anti–phospho-Src (Tyr^{527}), or anti-Src by stripping and reprobing of the same blots. Intensities of the bands were quantified with densitometric imager. The bar graphs are expressed relative to control value corrected by Src level (means ± SE). *$P < 0.05$; †$P < 0.01$. Representative blot panels of four (*A*) or three (*B*) independent experiments are shown.

Signaling (Danvers, MA); and mouse anti–β-actin from Sigma (St. Louis, MO). Secondary antibodies used were horseradish peroxidase–conjugated anti-rabbit and mouse antibody (GE Healthcare). Band intensities were quantified with Multi Gauge software (Fujifilm, Tokyo, Japan).

Measurement of ROS production. ROS production in islet cells was measured by 2′,7′-dichlorofluorescein fluorescence (6). Briefly, cultured islets were dispersed using 0.05% trypsin/0.53 mmol/l EDTA (Invitrogen, Carlsbad, CA) and PBS. Dispersed islet cells were preincubated in KRBB medium containing 2.8 mmol/l glucose and 10 μmol/l 5-(and 6-) chloromethyl-2′,7′-dichlorodihydrofluorescein diacetate (CM-H_2DCFDA; Invitrogen) for 20 min at 37°C. After a 60-min incubation in 400 μl KRBB medium containing 16.7 mmol/l glucose with or without test materials, fluorescence was measured using a spectrofluorophotometer (RF-5300PC; Shimadzu, Kyoto, Japan), with excitation wavelength at 505 nm and emission wavelength at 540 nm. Fluorescence was corrected by subtracting parallel blanks and represented by fold increases of the value at time zero.

Measurement of ATP content. ATP content in islets was determined by luminometry as previously described (6). Briefly, after preincubation, groups of 10 islets were batch incubated for 30 min in KRBB medium containing 2.8 or 16.7 mmol/l glucose with or without test materials. Incubation was stopped immediately by addition of $HClO_4$ and sonication in ice-cold water for 10 min. They were then centrifuged, and a fraction of the supernatant was mixed with HEPES and Na_2CO_3. The ATP content in the supernatant of islet lysates was measured using ENLITEN luciferase/luciferin reagent (Promega, Madison, WI) with a luminometer (GloMax 20/20n; Promega).

Materials. Exendin-4 and forskolin were purchased from Sigma. PP2 was purchased from Tocris (Ellisville, MO). PP3, H-89, myristoylated PKA inhibitor amide14–22 (PKI), LY294002, wortmannin, PD98059, and AG1478 were purchased from Calbiochem. Dibutyryl cAMP was purchased from Daiichisankyo (Tokyo, Japan). 8-(4-chlorophenylthio)-2′-*O*-methyl-cAMP (8CPT-2Me-cAMP) was purchased from Biolog Life Science (Bremen, Germany).

Statistical analysis. Data are expressed as means ± SE. Statistical significance of difference was evaluated by the unpaired Student *t* test. $P < 0.05$ was considered significant.

RESULTS

Comparison of expression of Src between Wistar and GK islets. To examine whether the expression levels of Src in GK islets differ from those in Wistar islets, immunoblotting using fresh islets was performed. As shown in Fig. 1*A*, the level of Src pY416, which indicates activation of Src, in GK islets was significantly higher than that in Wistar islets. The levels of Src pY527, total Src, and Csk in GK islets were significantly lower than those in Wistar islets. The levels of other Src family kinases (SFKs) were similar in Wistar and GK islets, whereas the expression of Fgr was very low and that of Fyn was undetectable (supplementary Fig. 1 in the online appendix, available at http://diabetes.diabetesjournals.org/cgi/content/full/db10-0021/DC1). Results of immunoblotting using islets cultured for 20 h in the presence of 5.5 mmol/l glucose (supplementary Fig. 2) were similar to those shown in Fig. 1*A*.

Exendin-4 suppresses Src activity in GK islets. To investigate whether exendin-4 regulates Src activity, phosphorylation of Src was examined by immunoprecipitation and immunoblotting. As shown in Fig. 2*A*, Src pY416 was

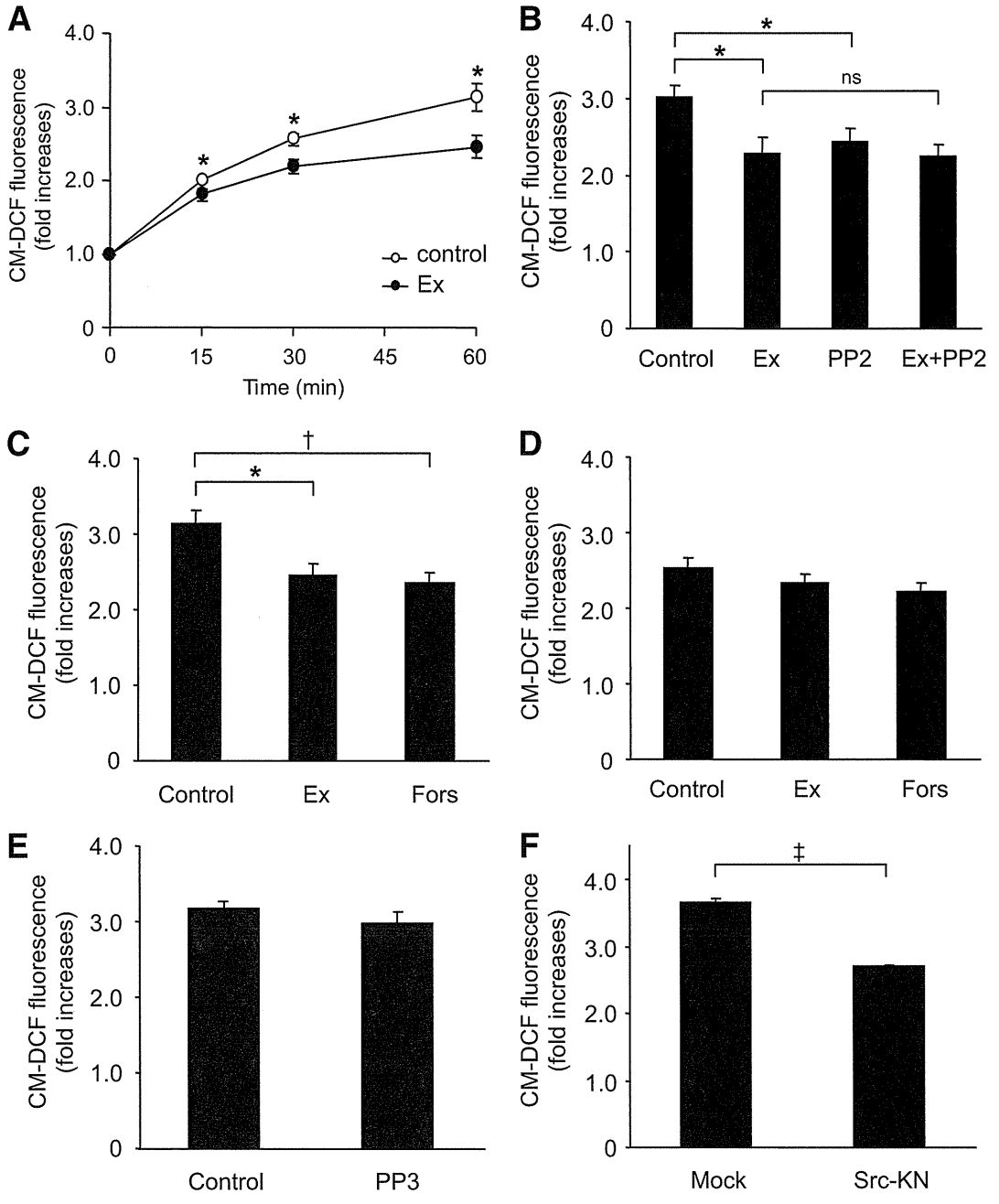

FIG. 3. Exendin-4 decreases ROS production at high glucose in GK islet cells. *A*: Time course of high-glucose–induced ROS production with or without 100 nmol/l exendin-4 in GK islet cells. After preincubation in the presence of 2.8 mmol/l glucose and 10 μmol/l CM-H_2DCFDA for 20 min, dispersed islet cells were incubated in the presence of 16.7 mmol/l glucose with (●) or without (○) 100 nmol/l exedin-4 for 60 min. Fluorescence is represented as fold increases against the value at time zero. Data are expressed as means ± SE (n = 5–7). *P < 0.05 vs. control. *B*: Effects of exendin-4 and PP2 on high-glucose–induced ROS production at 60 min in GK islet cells. Data are expressed as means ± SE (n = 4–6). *P < 0.05. *C*: Effects of exendin-4 and forskolin on high-glucose–induced ROS production at 60 min in GK islet cells. Data are expressed as means ± SE (n = 5–6). *P < 0.05; †P < 0.01. *D*: Effects of exendin-4 and forskolin on high-glucose–induced ROS production at 60 min in Wistar islet cells. Data are expressed as means ± SE (n = 3–4). *E*: Effects of PP3 on high-glucose–induced ROS production at 60 min in GK islet cells. Data are expressed as means ± SE (n = 3). *F*: Effect of Src-KN on high-glucose–induced ROS production at 60 min in GK islet cells. Retroviral (empty vector and Src-KN vector)-mediated gene transfer to islets was carried out by in vivo gene transduction method, as described in RESEARCH DESIGN AND METHODS. Data are expressed as means ± SE (n = 3). ‡P < 0.001.

significantly decreased by 100 nmol/l exendin-4 in the presence of 16.7 mmol/l glucose in GK islets. Exendin-4 also significantly increased Src pY527 in GK islets in the same condition. On the other hand, exendin-4 did not affect Src pY416 or pY527 at high glucose in Wistar islets (Fig. 2*B*). Both Src pY416 and pY527 were not altered by change in glucose concentration in GK or Wistar islets (supplementary Fig. 3).

Exendin-4 decreases ROS production in GK islet cells. We then investigated whether exendin-4 ameliorates endogenous ROS production at high glucose in GK islet cells. A total of 16.7 mmol/l glucose exposure induced ROS production in GK islet cells (Fig. 3*A*). Coexposure of exendin-4 significantly decreased ROS production in the presence of 16.7 mmol/l glucose at 15, 30, and 60 min. A total of 10 μmol/l PP2, a Src inhibitor, significantly de-

creased high-glucose–induced ROS production (Fig. 3*B*), but PP3, the inactive PP2 analog, did not affect it (Fig. 3*E*). Exendin-4 did not further decrease ROS production in the presence of PP2 (Fig. 3*B*), suggesting that the effect of exendin-4 is via the Src signal. The decrease in high-glucose–induced ROS production also was observed in the presence of 10 μmol/l forskolin, an adenylyl cyclase activator (Fig. 3*C*). High-glucose–induced ROS production in Wistar islet cells was lower than that in GK islet cells and was not changed by addition of exendin-4 or forskolin (Fig. 3*D*). To confirm that Src is actually involved in ROS production, we measured ROS production in GK islets expressing a kinase-negative form of Src (Src-KN) by retroviral vector. ROS production in Src-KN–expressing islets was significantly lower than that in control (Fig. 3*F*), demonstrating that Src regulates ROS production in GK islets.

Exendin-4 increases ATP content in GK islets. In Wistar islets, 16.7 mmol/l glucose-exposure significantly increased ATP content compared with that in the presence of 2.8 mmol/l glucose, as shown in Fig. 4*B*. Exendin-4, PP2, or exendin-4 plus PP2 did not affect the ATP content in the presence of 16.7 mmol/l glucose in Wistar islets. The ATP content in GK islets exposed to 16.7 mmol/l glucose was not increased compared with that in the presence of 2.8 mmol/l glucose (Fig. 4*A*). Exendin-4 as well as PP2 significantly increased the ATP content in the presence of 16.7 mmol/l glucose. Further increase of ATP content by combined exendin-4 and PP2 was not observed.

The effects of exendin-4 are dependent on Epac. We then investigated whether the decrease in ROS production by exendin-4 is dependent on PKA. As shown in Fig. 5*A*, decreased ROS production by exendin-4 or forskolin was not affected by 10 μmol/l H-89 or PKI, a PKA inhibitor, indicating that the effect is PKA independent. Not only dibutyryl cAMP, a general cAMP analog, but also 8CPT-2Me-cAMP, an Epac-specific cAMP analog, decreased ROS production (Fig. 5*C*). Epac possesses guanine nucleotide exchange factor activity toward Rap1, a member of the Ras superfamily of small GTPases. Epac2 and Rap1 proteins were expressed similarly in both Wistar and GK islets (Fig. 5*B*). To determine involvement of Epac in Src activation, Src phosphorylation was examined. Src pY416 was significantly decreased by 8CPT-2Me-cAMP (Fig. 5*D*).

A downstream pathway of Src is PI3K/Akt signaling. Src signalings toward downstream proteins are complex, but one of the typical pathways is phosphatidylinositol 3 kinase (PI3K)/Akt signaling (8). We therefore examined the involvement of PI3K/Akt signaling on ROS production. A total of 50 μmol/l LY294002 and 0.5 μmol/l wortmannin, both of which are PI3K inhibitors, significantly decreased ROS production in GK islets (Fig. 6*A*). Exendin-4 and PP2 both significantly decreased phosphorylation of Akt in GK islets (Fig. 6*B*) but not in Wistar islets (Fig. 6*C*). Considering these findings together, PI3K/Akt signaling that produces ROS is located downstream of Src activation. We also examined the involvement of mitogen-activated protein kinase signaling, another downstream pathway of Src. A total of 50 μmol/l PD98059, a MAPK-ERK kinase inhibitor, did not affect ROS production in GK islets (Fig. 6*D*), and neither exendin-4 nor PP2 affected phosphorylation of ERK (Fig. 6*E*). Several GPCR agonists have been shown to induce transactivation of epidermal growth factor receptor (EGFR) (24,25) by a mechanism involving Src (25–27) and frequently subsequent PI3K/Akt signaling (25,28). Therefore, involvement of EGFR transactivation on regulation of ROS production was examined. A total of 0.5 μmol/l AG1478, an EGFR kinase inhibitor, significantly decreased ROS production (Fig. 6*F*).

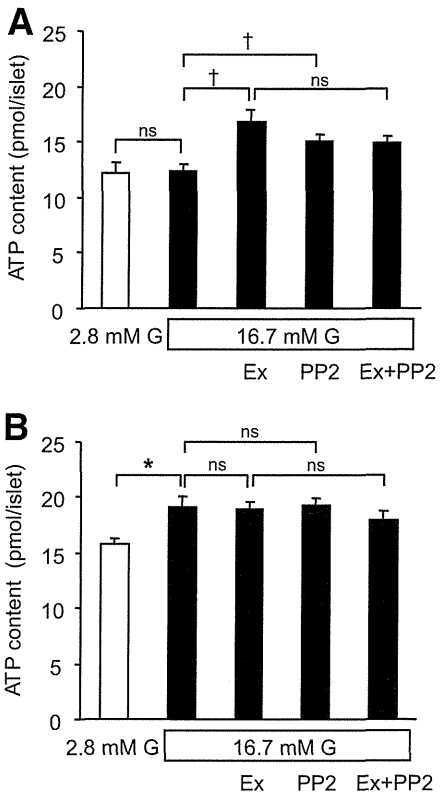

FIG. 4. Exendin-4 increases ATP content at high glucose in GK islets. Effects of exendin-4 and PP2 on ATP content in the presence of high glucose for 30 min in GK (*A*) and Wistar (*B*) islets. After preincubation in the presence of 2.8 mmol/l glucose for 30 min, islets were incubated in the presence of 2.8 or 16.7 mmol/l glucose with or without 100 nmol/l exendin-4, 10 μmol/l PP2, or both for 30 min. Data are expressed as means ± SE (n = 7–8). *P < 0.05; †P < 0.01.

DISCUSSION

We previously reported that endogenous ROS production by high glucose in diabetic GK islets is elevated compared with that in control Wistar islets and is effectively ameliorated by Src inhibition, suggesting that Src may be activated in GK islets (6). In the present study, we first investigated whether Src activity is altered in GK islets. Immunoblotting analysis revealed that the level of Src pY416, which indicates the level of Src activation, is higher in GK islets than that in Wistar islets, despite lower levels of total Src, Src pY527, and Csk. The lower level of total Src seems to be a consequence of Src activation. Targeted degradation of active forms of Src is brought about by ubiquitination (29). The protooncogene c-Cbl, recently found to be an E3 ubiquitin ligase, mediates ubiquitination of activated Src (30). These reports suggest that increased degradation of activated Src may result in a lower level of total Src in GK islets. In addition, a lower level of Csk might cause a lower activity of the kinase in GK islets. However, Src activity is not directly regulated through phosphorylation of Tyr527 by Csk (8), and a subtle decrease in Csk activity is not believed to contribute to regulation of Src activity because of the excess amount of expression of Csk. This is supported by the findings that heterozygous disruption of ubiquitously expressed Csk

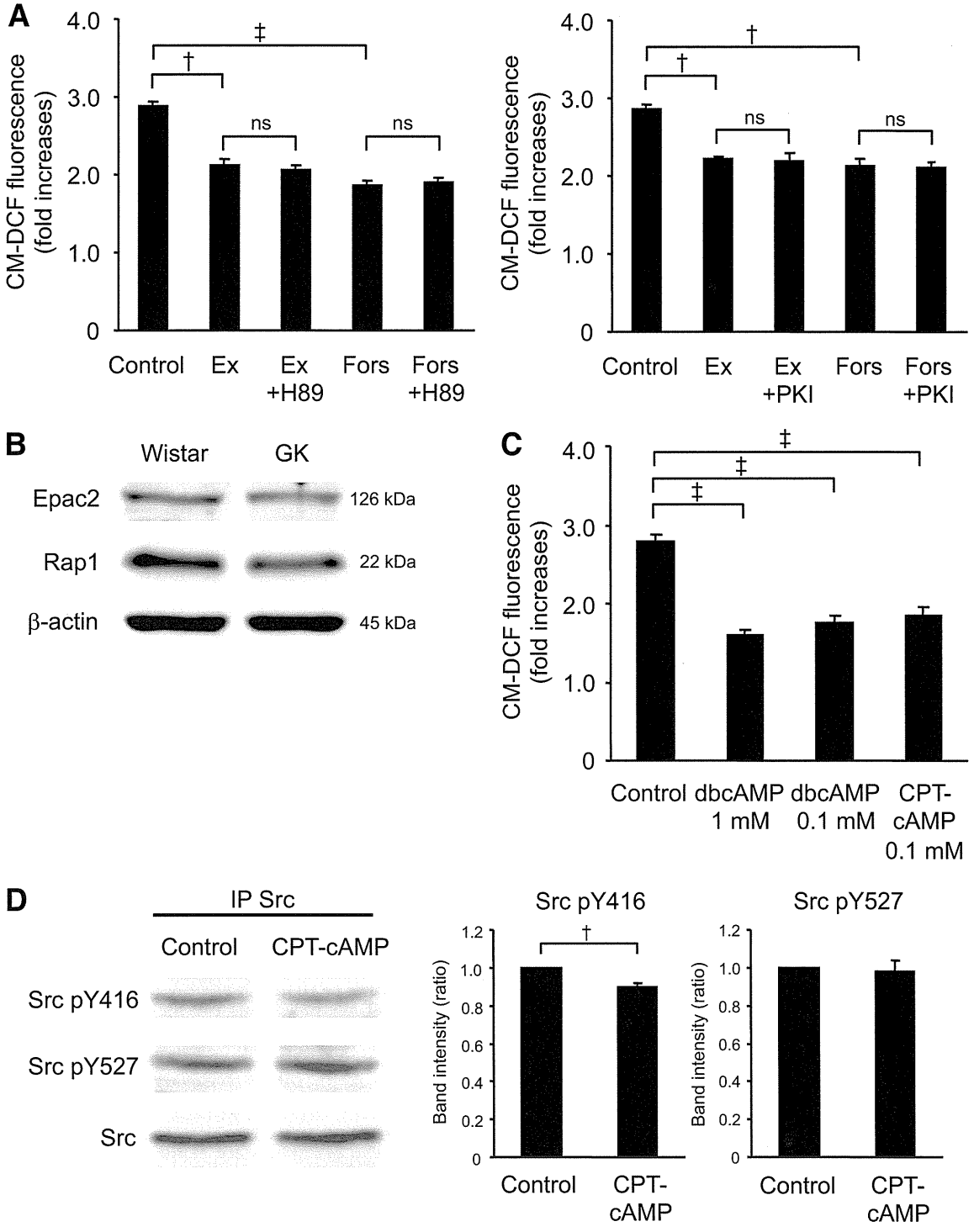

FIG. 5. The effects of exendin-4 are dependent not on PKA but on Epac. *A*: **Effects of H-89 or PKI on the decrease in high-glucose–induced ROS production by exendin-4 or forskolin at 60 min in GK islet cells. After preincubation in the presence of 2.8 mmol/l glucose and 10 μmol/l CM-H_2DCFDA for 20 min, dispersed islet cells were incubated in the presence of 16.7 mmol/l glucose with or without 100 nmol/l exendin-4 or 10 μmol/l forskolin with or without 10 μmol/l H-89 or 10 μmol/l PKI for 60 min. Fluorescence is represented as fold increases against the value at time zero. Data are expressed as means ± SE (n = 3). †P < 0.01; ‡P < 0.001.** *B*: **Expression of Epac2 and Rap1 in Wistar and GK islets. Fresh islets were lysated and subjected to immunoblot analyses. Blots (50 μg of protein) were probed with anti-Epac2 or anti-Rap1. The same blots were stripped and reprobed with anti–β-actin, respectively. Representative blot panels of three independent experiments are shown.** *C*: **Effects of cAMP analogs on high-glucose–induced ROS production at 60 min in GK islet cells. Data are expressed as means ± SE (n = 3–4). ‡P < 0.001.** *D*: **Epac-specific cAMP analog suppresses Src activity at high glucose in GK islets. After preincubation in the presence of 2.8 mmol/l glucose for 30 min, islets were incubated in the presence of 16.7 mmol/l glucose with or without 0.1 mmol/l 8CPT-2Me-cAMP for 8 min. Islet lysates (~2 mg of protein) were immunoprecipitated with anti-Src antibody and subjected to immunoblot analyses. Blots were probed with anti–phospho-Src (Tyr^{416}), anti–phospho-Src (Tyr^{527}), or anti-Src by stripping and reprobing of the same blots. Intensities of the bands were quantified with densitometric imager. The bar graphs are expressed relative to control value corrected by Src level (means ± SE). †P < 0.01. Representative blot panels of four independent experiments are shown.**

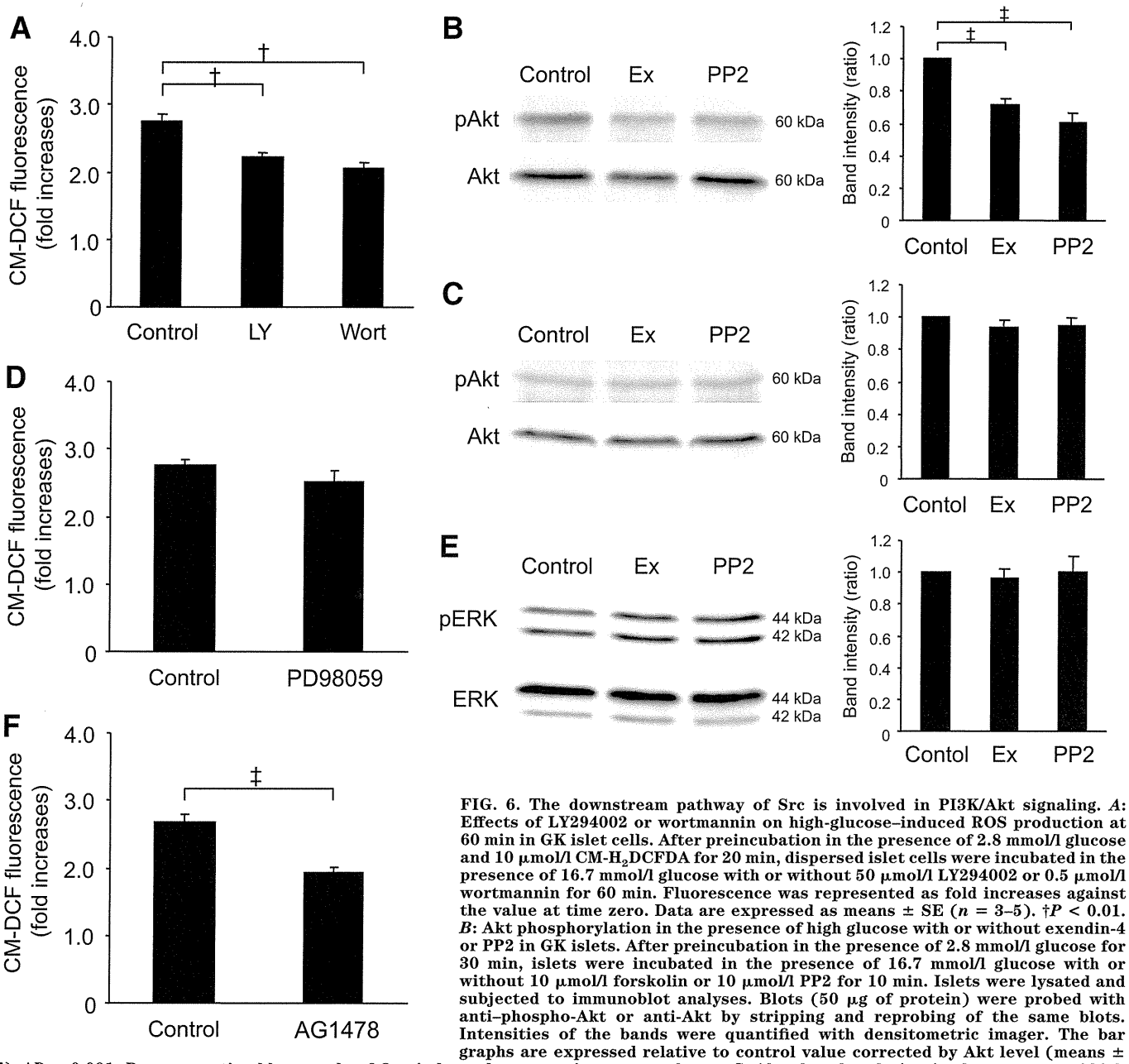

FIG. 6. The downstream pathway of Src is involved in PI3K/Akt signaling. *A*: Effects of LY294002 or wortmannin on high-glucose–induced ROS production at 60 min in GK islet cells. After preincubation in the presence of 2.8 mmol/l glucose and 10 μmol/l CM-H_2DCFDA for 20 min, dispersed islet cells were incubated in the presence of 16.7 mmol/l glucose with or without 50 μmol/l LY294002 or 0.5 μmol/l wortmannin for 60 min. Fluorescence was represented as fold increases against the value at time zero. Data are expressed as means ± SE (n = 3–5). †P < 0.01. *B*: Akt phosphorylation in the presence of high glucose with or without exendin-4 or PP2 in GK islets. After preincubation in the presence of 2.8 mmol/l glucose for 30 min, islets were incubated in the presence of 16.7 mmol/l glucose with or without 10 μmol/l forskolin or 10 μmol/l PP2 for 10 min. Islets were lysated and subjected to immunoblot analyses. Blots (50 μg of protein) were probed with anti–phospho-Akt or anti-Akt by stripping and reprobing of the same blots. Intensities of the bands were quantified with densitometric imager. The bar graphs are expressed relative to control value corrected by Akt level (means ± SE). ‡P < 0.001. Representative blot panels of five independent experiments are shown. *C*: Akt phosphorylation in the presence of high glucose with or without exendin-4 or PP2 in Wistar islets. Representative blot panels of three independent experiments are shown. *D*: Effects of PD98059 on high-glucose–induced ROS production at 60 min in GK islet cells. Data are expressed as means ± SE (n = 4). *E*: ERK phosphorylation in the presence of high glucose with or without exendin-4 or PP2 in GK islets. Blots (50 μg of protein) were probed with anti–phospho-ERK or anti-ERK by stripping and reprobing of the same blots. The bar graphs are expressed relative to control value corrected by ERK level (means ± SE). Representative blot panels of three independent experiments are shown. *F*: Effects of AG1478 on high-glucose–induced ROS production at 60 min in GK islet cells. Data are expressed as means ± SE (n = 5). ‡P < 0.001.

does not affect the phenotype in mice, contrary to neural tube defects and embryonic lethality in homozygous deficient mice (31). Moreover, the localization of Csk in the cytosol before recruitment to the membrane for Src regulation dose not differ in Wistar and GK islets (supplementary Fig. 4). Thus, the lower expression level of Csk found in our results is not likely to play a role in the Src activation in GK islets. Activation of Src as well as elevated endogenous ROS production at high glucose in GK islets was clearly suppressed by exendin-4, which did not affect Src phosphorylation or ROS production in Wistar islets. Thus, the GLP-1 signal might well suppress activation of Src and excessive ROS production under diabetic conditions in addition to other beneficial long-term effects on β-cells.

GLP-1 induces elevation of intracellular cAMP levels and subsequent activation of PKA after binding to the GLP-1 receptor. In the present study, the effect of GLP-1 signaling, which suppresses Src activation and ROS production, was found to be independent of PKA. Epac is a PKA-independent cAMP sensor; Epac2 is expressed mainly in neuroendocrine cells including pancreatic β-cells. Epac2 regulates exocytosis of insulin granules in β-cells by mobilizing intracellular Ca^{2+} and interacting granule-associated proteins (14,15). Although the relationship between Epac and Src is not well known, a recent

report (32) has shown that cAMP protects against hepatocyte apoptosis Epac dependently through Src and PI3K/Akt activation. Further evaluation of the role of cAMP in regulation of Src and PI3K/Akt signaling is required.

In the present study, we have shown that one of these Src signals, the PI3K/Akt signal, regulates ROS production. Furthermore, GLP-1 induces β-cell proliferation through PI3K signaling via Src and EGFR transactivation (33). Our finding that the EGFR kinase inhibitor decreases ROS production suggests that EGFR transactivation may be involved in the ROS-reducing effect of exendin-4 via Src. Under normal conditions, GPCR stimulation generally activates Src toward EGFR transactivation, frequently followed by PI3K activation (25). The present study reveals that Src and PI3K activities are upregulated in islets under diabetic conditions, which are suppressed by the GLP-1 signal. Many studies in oncology have shown that several growth factors including EGF and platelet-derived growth factor induce ROS through PI3K activation (34–36). Thus, EGFR transactivation/PI3K signaling should be activated under pathophysiologically disordered conditions. In the various states between normal and diabetic conditions, the ameliorative effects of the GLP-1 signal may differ (37). Further elucidation of these signals in the pathophysiology of diabetes should be helpful in future development of therapeutic strategies.

Previous studies have shown that the antioxidant capacity in β-cells is very low because of weak expression of antioxidant enzymes in pancreatic islets compared with that in various other tissues (38). The superoxide anion is converted by superoxide dismutase (SOD) into hydrogen peroxide that is eventually removed by glutathione peroxidase (Gpx). The expression level of MnSOD, which is localized in mitochondria, was significantly lower in GK islets than in Wistar islets, and that of of Gpx was similar in Wistar and GK islets (supplementaty Fig. 5*A*). However, an enzymatic assay revealed that MnSOD activity in GK islets was similar to that in Wistar islets and that it was not affected by exendin-4 or PP2 (supplementary Fig. 5*B* and *C*). These results indicate that regulation of MnSOD activity does not play a role in the suppressive effects of ROS production by exendin-4.

One of the important sites of ROS generation in β-cells is the mitochondrial electron transport chain, in which ROS generation increases according to the hyperpolarization of mitochondrial inner membrane derived from accelerated glucose metabolism (39). However, in pathophysiological conditions, NADPH oxidase may play an important role in ROS generation in β-cells. Chronic exposure to proinflammatory cytokines and abundant nutrients including glucose and palmitate augments the expression of a phagocyte-like NADPH oxidase in β-cells (40). Moreover, the expression of NADPH oxidase is increased in islets of diabetic Otsuka Long Evans Tokushima Fatty rats (41). Because Src is involved in regulation of NADPH oxidase activity (42), further examination to elucidate the site of ROS generation related to Src activation in β-cells is needed. On the other hand, previous reports have shown that ROS itself regulates Src activity (43,44) in addition to Src activity regulation of ROS production (45). To clarify this mutual causal relationship between Src and ROS, we examined ROS production in GK islets expressing Src-KN, which was found to cause a distinct decrease in high-glucose–induced ROS production. This finding demonstrates that Src activity regulates ROS production and does not contradict the possibility of a feedback regulation mechanism of ROS on Src activity (45).

The high-glucose–induced increase in ATP production is impaired in GK rats (6,46) as well as in patients with type 2 diabetes (47). In addition, islets in GK rats and human type 2 diabetes are oxidatively stressed (48–50). In the present study, exendin-4 was able to recover this impaired increase in ATP production by high glucose in GK islets as well as to decrease excessive ROS production. Thus, GLP-1 signaling may improve β-cell function in the diabetic state not only because it enhances Ca^{2+} efficacy of the exocytotic system of insulin granules but also because it improves impaired metabolism-secretion coupling. GLP-1 receptor agonists are widely used in treatment of type 2 diabetes for their ability to improve glucose intolerance. Their clinical beneficial effect seems to be provided not only by their insulinotropic action but also by their reduction of β-cell apoptosis and induction of β-cell proliferation (16–18). Further elucidation of endogenous ROS regulation by GLP-1 may help to clarify the mechanism of the various beneficial effects of these agents.

ACKNOWLEDGMENTS

This work was supported by a research grant on Nanotechnical Medicine from the Ministry of Health, Labor, and Welfare of Japan; by scientific research grants from the Ministry of Education, Culture, Sports, Science, and Technology of Japan; and also by the Kyoto University Global Center of Excellence Program Center for Frontier Medicine.

No potential conflicts of interest relevant to this article were reported.

E.M. researched data, contributed to the discussion, wrote the manuscript, and reviewed/edited the manuscript. S.F. contributed to the discussion, wrote the manuscript, and reviewed/edited the manuscript. H.S., C.O., R.K., Y.S., M.S., and Y.N. researched data. M.O. contributed to the discussion and reviewed/edited the manuscript. N.I. contributed to the discussion and reviewed/edited the manuscript.

Parts of this study were presented in abstract form at the 70th Scientific Sessions of the American Diabetes Association, Orlando, Florida, 25–29 June 2010.

We acknowledge the editorial assistance of Dalmen Mayer. We thank C. Kotake for excellent technical assistance.

REFERENCES

1. Maechler P, Wollheim CB. Mitochondrial function in normal and diabetic beta-cells. Nature 2001;414:807–812
2. Krippeit-Drews P, Kramer C, Welker S, Lang F, Ammon HP, Drews G. Interference of H2O2 with stimulus-secretion coupling in mouse pancreatic beta-cells. J Physiol 1999;514(Pt 2):471–481
3. Maechler P, Jornot L, Wollheim CB. Hydrogen peroxide alters mitochondrial activation and insulin secretion in pancreatic beta cells. J Biol Chem 1999;274:27905–27913
4. Bindokas VP, Kuznetsov A, Sreenan S, Polonsky KS, Roe MW, Philipson LH. Visualizing superoxide production in normal and diabetic rat islets of Langerhans. J Biol Chem 2003;278:9796–9801
5. Sakai K, Matsumoto K, Nishikawa T, Suefuji M, Nakamaru K, Hirashima Y, Kawashima J, Shirotani T, Ichinose K, Brownlee M, Araki E. Mitochondrial reactive oxygen species reduce insulin secretion by pancreatic beta-cells. Biochem Biophys Res Commun 2003;300:216–222
6. Kominato R, Fujimoto S, Mukai E, Nakamura Y, Nabe K, Shimodahira M, Nishi Y, Funakoshi S, Seino Y, Inagaki N. Src activation generates reactive oxygen species and impairs metabolism-secretion coupling in diabetic Goto-Kakizaki and ouabain-treated rat pancreatic islets. Diabetologia 2008;51:1226–1235
7. Xu W, Harrison SC, Eck MJ. Three-dimensional structure of the tyrosine kinase c-Src. Nature 1997;385:595–602

8. Martin GS. The hunting of the Src. Nat Rev Mol Cell Biol 2001;2:467–475
9. Nada S, Okada M, MacAuley A, Cooper JA, Nakagawa H. Cloning of a complementary DNA for a protein-tyrosine kinase that specifically phosphorylates a negative regulatory site of p60c-src. Nature 1991;351: 69–72
10. Baggio LL, Drucker DJ. Biology of incretins: GLP-1 and GIP. Gastroenterology 2007;132:2131–2157
11. Holst JJ. The physiology of glucagon-like peptide 1. Physiol Rev 2007;87: 1409–1439
12. Seino S, Shibasaki T. PKA-dependent and PKA-independent pathways for cAMP-regulated exocytosis. Physiol Rev 2005;85:1303–1342
13. Roscioni SS, Elzinga CR, Schmidt M. Epac: effectors and biological functions. Naunyn Schmiedebergs Arch Pharmacol 2008;377:345–357
14. Ozaki N, Shibasaki T, Kashima Y, Miki T, Takahashi K, Ueno H, Sunaga Y, Yano H, Matsuura Y, Iwanaga T, Takai Y, Seino S. cAMP-GEFII is a direct target of cAMP in regulated exocytosis. Nat Cell Biol 2000;2:805–811
15. Kang G, Joseph JW, Chepurny OG, Monaco M, Wheeler MB, Bos JL, Schwede F, Genieser HG, Holz GG. Epac-selective cAMP analog 8-pCPT-2′-O-Me-cAMP as a stimulus for Ca2+-induced Ca2+ release and exocytosis in pancreatic beta-cells. J Biol Chem 2003;278:8279–8285
16. Xu G, Stoffers DA, Habener JF, Bonner-Weir S. Exendin-4 stimulates both β-cell replication and neogenesis, resulting in increased β-cell mass and improved glucose tolerance in diabetic rats. Diabetes 1999; 48:2270–2276
17. Farilla L, Hui H, Bertolotto C, Kang E, Bulotta A, Di Mario U, Perfetti R. Glucagon-like peptide-1 promotes islet cell growth and inhibits apoptosis in Zucker diabetic rats. Endocrinology 2002;143:4397–4408
18. Li Y, Hansotia T, Yusta B, Ris F, Halban PA, Drucker DJ. Glucagon-like peptide-1 receptor signaling modulates beta cell apoptosis. J Biol Chem 2003;278:471–478
19. Tsunekawa S, Yamamoto N, Tsukamoto K, Itoh Y, Kaneko Y, Kimura T, Ariyoshi Y, Miura Y, Oiso Y, Niki I. Protection of pancreatic beta-cells by exendin-4 may involve the reduction of endoplasmic reticulum stress; in vivo and in vitro studies. J Endocrinol 2007;193:65–74
20. Cheng Q, Law PK, de Gasparo M, Leung PS. Combination of the dipeptidyl peptidase IV inhibitor LAF237 [(S)-1-[(3-hydroxy-1-adamantyl)amino]acetyl-2-cyanopyrrolidine] with the angiotensin II type 1 receptor antagonist valsartan [N-(1-oxopentyl)-N-[[2′-(1H-tetrazol-5-yl)-[1,1′-biphenyl]-4-yl]methyl]-L-valine] enhances pancreatic islet morphology and function in a mouse model of type 2 diabetes. J Pharmacol Exp Ther 2008;327:683–691
21. Akagi T, Sasai K, Hanafusa H. Refractory nature of normal human diploid fibroblasts with respect to oncogene-mediated transformation. Proc Natl Acad Sci U S A 2003;100:13567–13572
22. Florio M, Wilson LK, Trager JB, Thorner J, Martin GS. Aberrant protein phosphorylation at tyrosine is responsible for the growth-inhibitory action of pp60v-src expressed in the yeast Saccharomyces cerevisiae. Mol Biol Cell 1994;5:283–296
23. Mukai E, Fujimoto S, Sakurai F, Kawabata K, Yamashita M, Inagaki N, Mizuguchi H. Efficient gene transfer into murine pancreatic islets using adenovirus vectors. J Control Release 2007;119:136–141
24. Daub H, Weiss FU, Wallasch C, Ullrich A. Role of transactivation of the EGF receptor in signalling by G-protein-coupled receptors. Nature 1996; 379:557–560
25. Rozengurt E. Mitogenic signaling pathways induced by G protein-coupled receptors. J Cell Physiol 2007;213:589–602
26. Eguchi S, Iwasaki H, Inagami T, Numaguchi K, Yamakawa T, Motley ED, Owada KM, Marumo F, Hirata Y. Involvement of PYK2 in angiotensin II signaling of vascular smooth muscle cells. Hypertension 1999;33:201–206
27. Gao Y, Tang S, Zhou S, Ware JA. The thromboxane A2 receptor activates mitogen-activated protein kinase via protein kinase C-dependent Gi coupling and Src-dependent phosphorylation of the epidermal growth factor receptor. J Pharmacol Exp Ther 2001;296:426–433
28. Chiu T, Santiskulvong C, Rozengurt E. EGF receptor transactivation mediates ANG II-stimulated mitogenesis in intestinal epithelial cells through the PI3-kinase/Akt/mTOR/p70S6K1 signaling pathway. Am J Physiol Gastrointest Liver Physiol 2005;288:G182–G194
29. Harris KF, Shoji I, Cooper EM, Kumar S, Oda H, Howley PM. Ubiquitin-mediated degradation of active Src tyrosine kinase. Proc Natl Acad Sci U S A 1999;96:13738–13743
30. Yokouchi M, Kondo T, Sanjay A, Houghton A, Yoshimura A, Komiya S, Zhang H, Baron R. Src-catalyzed phosphorylation of c-Cbl leads to the interdependent ubiquitination of both proteins. J Biol Chem 2001;276: 35185–35193
31. Nada S, Yagi T, Takeda H, Tokunaga T, Nakagawa H, Ikawa Y, Okada M, Aizawa S. Constitutive activation of Src family kinases in mouse embryos that lack Csk. Cell 1993;73:1125–1135
32. Gates A, Hohenester S, Anwer MS, Webster CR. cAMP-GEF cytoprotection by Src tyrosine kinase activation of phosphoinositide-3-kinase p110 beta/alpha in rat hepatocytes. Am J Physiol Gastrointest Liver Physiol 2009;296: G764–G774
33. Buteau J, Foisy S, Joly E, Prentki M. Glucagon-like peptide 1 induces pancreatic β-cell proliferation via transactivation of the epidermal growth factor receptor. Diabetes 2003;52:124–132
34. Zhu QS, Xia L, Mills GB, Lowell CA, Touw IP, Corey SJ. G-CSF induced reactive oxygen species involves Lyn-PI3-kinase-Akt and contributes to myeloid cell growth. Blood 2006;107:1847–1856
35. Baumer AT, Ten Freyhaus H, Sauer H, Wartenberg M, Kappert K, Schnabel P, Konkol C, Hescheler J, Vantler M, Rosenkranz S. Phosphatidylinositol 3-kinase-dependent membrane recruitment of Rac-1 and p47phox is critical for alpha-platelet-derived growth factor receptor-induced production of reactive oxygen species. J Biol Chem 2008;283:7864–7876
36. Binker MG, Binker-Cosen AA, Richards D, Oliver B, Cosen-Binker LI. EGF promotes invasion by PANC-1 cells through Rac1/ROS-dependent secretion and activation of MMP-2. Biochem Biophys Res Commun 2009;379: 445–450
37. Peyot ML, Gray JP, Lamontagne J, Smith PJ, Holz GG, Madiraju SR, Prentki M, Heart E. Glucagon-like peptide-1 induced signaling and insulin secretion do not drive fuel and energy metabolism in primary rodent pancreatic beta-cells. PLoS One 2009;4:e6221
38. Tiedge M, Lortz S, Drinkgern J, Lenzen S. Relation between antioxidant enzyme gene expression and antioxidative defense status of insulin-producing cells. Diabetes 1997;46:1733–1742
39. Newsholme P, Haber EP, Hirabara SM, Rebelato EL, Procopio J, Morgan D, Oliveira-Emilio HC, Carpinelli AR, Curi R. Diabetes associated cell stress and dysfunction: role of mitochondrial and non-mitochondrial ROS production and activity. J Physiol 2007;583:9–24
40. Morgan D, Oliveira-Emilio HR, Keane D, Hirata AE, Santos da Rocha M, Bordin S, Curi R, Newsholme P, Carpinelli AR. Glucose, palmitate and pro-inflammatory cytokines modulate production and activity of a phagocyte-like NADPH oxidase in rat pancreatic islets and a clonal beta cell line. Diabetologia 2007;50:359–369
41. Nakayama M, Inoguchi T, Sonta T, Maeda Y, Sasaki S, Sawada F, Tsubouchi H, Sonoda N, Kobayashi K, Sumimoto H, Nawata H. Increased expression of NAD(P)H oxidase in islets of animal models of Type 2 diabetes and its improvement by an AT1 receptor antagonist. Biochem Biophys Res Commun 2005;332:927–933
42. Chowdhury AK, Watkins T, Parinandi NL, Saatian B, Kleinberg ME, Usatyuk PV, Natarajan V. Src-mediated tyrosine phosphorylation of p47phox in hyperoxia-induced activation of NADPH oxidase and generation of reactive oxygen species in lung endothelial cells. J Biol Chem 2005;280:20700–20711
43. Giannoni E, Buricchi F, Raugei G, Ramponi G, Chiarugi P. Intracellular reactive oxygen species activate Src tyrosine kinase during cell adhesion and anchorage-dependent cell growth. Mol Cell Biol 2005;25:6391–6403
44. Zhang J, Xing D, Gao X. Low-power laser irradiation activates Src tyrosine kinase through reactive oxygen species-mediated signaling pathway. J Cell Physiol 2008;217:518–528
45. Xie Z, Cai T. Na+-K+-ATPase-mediated signal transduction: from protein interaction to cellular function. Mol Interv 2003;3:157–168
46. Hughes SJ, Faehling M, Thorneley CW, Proks P, Ashcroft FM, Smith PA. Electrophysiological and metabolic characterization of single β-cells and islets from diabetic GK rats. Diabetes 1998;47:73–81
47. Anello M, Lupi R, Spampinato D, Piro S, Masini M, Boggi U, Del Prato S, Rabuazzo AM, Purrello F, Marchetti P. Functional and morphological alterations of mitochondria in pancreatic beta cells from type 2 diabetic patients. Diabetologia 2005;48:282–289
48. Ihara Y, Toyokuni S, Uchida K, Odaka H, Tanaka T, Ikeda H, Hiai H, Seino Y, Yamada Y. Hyperglycemia causes oxidative stress in pancreatic β-cells of GK rats, a model of type 2 diabetes. Diabetes 1999;48:927–932
49. Sakuraba H, Mizukami H, Yagihashi N, Wada R, Hanyu C, Yagihashi S. Reduced beta-cell mass and expression of oxidative stress-related DNA damage in the islet of Japanese Type II diabetic patients. Diabetologia 2002;45:85–96
50. Del Guerra S, Lupi R, Marselli L, Masini M, Bugliani M, Sbrana S, Torri S, Pollera M, Boggi U, Mosca F, Del Prato S, Marchetti P. Functional and molecular defects of pancreatic islets in human type 2 diabetes. Diabetes 2005;54:727–735

Biochemical and Biophysical Research Communications 404 (2011) 115–120

Contents lists available at ScienceDirect

Biochemical and Biophysical Research Communications

journal homepage: www.elsevier.com/locate/ybbrc

The effect of gastric inhibitory polypeptide on intestinal glucose absorption and intestinal motility in mice

Eiichi Ogawa [a], Masaya Hosokawa [a,b], Norio Harada [a], Shunsuke Yamane [a], Akihiro Hamasaki [a], Kentaro Toyoda [a], Shimpei Fujimoto [a], Yoshihito Fujita [a], Kazuhito Fukuda [a], Katsushi Tsukiyama [a,c], Yuichiro Yamada [a,c], Yutaka Seino [a,d], Nobuya Inagaki [a,e,*]

[a] Department of Diabetes and Clinical Nutrition, Graduate School of Medicine, Kyoto University, Japan
[b] Faculty of Human Sciences, Tezukayama Gakuin University, Osaka, Japan
[c] Department of Internal Medicine, Division of Endocrinology, Diabetes and Geriatric Medicine, Akita University School of Medicine, Akita, Japan
[d] Kansai Electric Power Hospital, Osaka, Japan
[e] CREST of Japan Science and Technology Cooperation (JST), Kyoto, Japan

ARTICLE INFO

Article history:
Received 21 October 2010
Available online 21 November 2010

Keywords:
GIP
Glucose absorption
Intestine

ABSTRACT

Gastric inhibitory polypeptide (GIP) is released from the small intestine upon meal ingestion and increases insulin secretion from pancreatic β cells. Although the GIP receptor is known to be expressed in small intestine, the effects of GIP in small intestine are not fully understood. This study was designed to clarify the effect of GIP on intestinal glucose absorption and intestinal motility. Intestinal glucose absorption *in vivo* was measured by single-pass perfusion method. Incorporation of [^{14}C]-glucose into everted jejunal rings *in vitro* was used to evaluate the effect of GIP on sodium-glucose co-transporter (SGLT). Motility of small intestine was measured by intestinal transit after oral administration of a non-absorbed marker. Intraperitoneal administration of GIP inhibited glucose absorption in wild-type mice in a concentration-dependent manner, showing maximum decrease at the dosage of 50 nmol/kg body weight. In glucagon-like-peptide-1 (GLP-1) receptor-deficient mice, GIP inhibited glucose absorption as in wild-type mice. *In vitro* examination of [^{14}C]-glucose uptake revealed that 100 nM GIP did not change SGLT-dependent glucose uptake in wild-type mice. After intraperitoneal administration of GIP (50 nmol/kg body weight), small intestinal transit was inhibited to 40% in both wild-type and GLP-1 receptor-deficient mice. Furthermore, a somatostatin receptor antagonist, cyclosomatostatin, reduced the inhibitory effect of GIP on both intestinal transit and glucose absorption in wild-type mice. These results demonstrate that exogenous GIP inhibits intestinal glucose absorption by reducing intestinal motility through a somatostatin-mediated pathway rather than through a GLP-1-mediated pathway.

1. Introduction

Gastric inhibitory polypeptide (GIP), also called glucose-dependent insulinotropic polypeptide, is an incretin of 42-amino-acid polypeptide synthesized by K cells of the duodenum and small intestine [1]. We previously generated GIP receptor-deficient mice (GIPR$^{-/-}$ mice) and showed that GIPR$^{-/-}$ mice have higher blood glucose levels as well as impaired initial insulin response after oral glucose load [2]. Thus, early insulin secretion stimulated by GIP plays an important role in glucose tolerance after oral glucose load.

While GIP receptor mRNA was reported to be present in rat gut [3], the role of the GIP receptor in the gut has not been fully clarified. In this *in vivo* study, we investigated the effect of exogenous GIP on intestinal glucose absorption in mice using the intestinal perfusion method. We investigated the effect of exogenous GIP on SGLT-dependent glucose uptake *in vitro* by using the everted jejunal ring method. Because intestinal motility and absorption are positively related [4,5], we investigated the effect of exogenous GIP on gastrointestinal motility by non-absorbed marker method. Since SST secretion has been reported to be stimulated by GIP and to prolong intestinal motility, we also investigated the involvement of SST in the inhibitory effect of exogenous GIP on both intestinal transit and intestinal glucose absorption by using somatostatin receptor antagonist. Our results demonstrate that exogenous GIP inhibits intestinal glucose absorption by reducing intestinal motility through a somatostatin-mediated pathway rather than through a GLP-1-mediated pathway.

Abbreviations: GIP, Gastric inhibitory polypeptide; GLP-1, glucagon-like-peptide-1; SST, somatostatin; SGLT, sodium-glucose co-transporter; CSS, cyclosomatostatin.

* Corresponding author. Address: Department of Diabetes and Clinical Nutrition, Graduate School of Medicine, Kyoto University, 54 Shogoin, Kawahara-cho, Sakyo-ku, Kyoto 606-8507, Japan. Fax: +81 75 771 6601.
E-mail address: inagaki@metab.kuhp.kyoto-u.ac.jp (N. Inagaki).

0006-291X/$ - see front matter © 2010 Elsevier Inc. All rights reserved.
doi:10.1016/j.bbrc.2010.11.077

2. Materials and methods

2.1. Animals

Male C57/BL6J mice weighing 25–30 g (8–14 weeks old) were housed in a temperature (25 ± 2 °C)- and moisture (50%)-controlled room with a 12 h light/dark cycle (6:00 AM/6:00 PM). The mice were fed standard mouse chow (Oriental Yeast, Osaka) and tap water *ad libitium*, and used as wild-type mice.

Generation of GIPR$^{-/-}$ mice and GLP-1 receptor-deficient mice (GLP-1R$^{-/-}$ mice) was described previously [2,6]. GLP-1R$^{-/-}$ mice were kindly provided by Dr. Daniel J. Drucker [6]. Age-matched male GIPR$^{-/-}$ and GLP-1R$^{-/-}$ mice were used in the experiments. The Animal Care Committee of Kyoto University Graduate School of Medicine approved animal care and procedures.

2.2. Materials

Synthetic human GIP was purchased from Peptide Institute (Osaka, Japan). The somatostatin receptor antagonist, cyclo(7-aminoheptanoyl-PHE-D-TRP-LYS-THR(BZL)) (cyclosomatostatin (CSS)) and somatostatin 28 (SST) were from Sigma Chemical Co. (St. Louis, MO). All other chemicals were of reagent grade.

2.3. Perfusion experiment

Single-pass perfusion method [7] was used to measure the effect of exogenous GIP or SST on intestinal glucose absorption using C57/BL6J mice. Preperfusion was done for a 45 min equilibration period and the samples were discarded. Three 15 min samples were then collected. GIP or SST was administered intraperitoneally at 60 min after starting the preperfusion according to the protocol (Fig. 1A). The change of absorption was calculated as the glucose concentration of the first sample collected (Period 1) minus the glucose concentration of the last sample collected (Period 2), and expressed as per centimeter perfused bowel. Negative values indicate an inhibitory effect on absorption; positive values indicate an increased effect on absorption.

2.4. Glucose uptake in jejunum in vitro

Incorporation of D-glucose into everted jejunal rings was determined as described previously [8]. SGLT-dependent glucose uptake for 15 min was determined as the glucose uptake in the absence of phlorizin minus the glucose uptake in the presence of phlorizin.

2.5. Small intestinal transit after intraperitoneal administration of GIP

Transit through the stomach and small intestine was measured by administering a non-absorbed marker containing 10% charcoal suspension in 5% gum Arabic, as previously described [9]. The mice were given 0.2 ml of the suspension by gavage through a straight blunt-ended feeding needle. GIP (50 nmol/kg body weight) or SST (75 nmol/kg body weight) or vehicle (saline) was administered intraperitoneally 15 min prior to the administration of the non-absorbed marker. CSS (1 μg/kg body weight), or vehicle (saline) was intraperitoneally administered 10 min prior to GIP administration.

2.6. Plasma GIP and SST assays

Blood was collected from the tail vein before the intraperitoneal administration of GIP (50 nmol/kg body weight) and collected again 20 min after the administration. ELISA assay kit was used according to the manufacture's instruction for the determination of plasma total GIP concentration (Linco Research, St. Charles, MO) and SST concentration (Phoenix Pharmaceuticals INC., Belmont, CA), respectively.

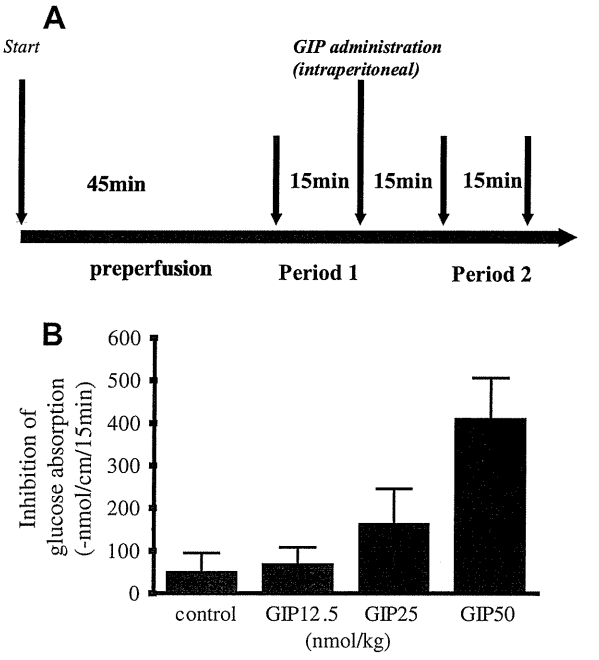

Fig. 1. (A) Diagram showing the sampling protocol of intestinal perfusion. The flow rate of the perfusion fluid was 2 ml/15 min. Perfusion began with an equilibration period of 45 min, which samples were discarded. The samples of Period 1 and Period 2 were then collected. GIP was administered intraperitoneally 60 min after the beginning of preperfusion. The change of absorption was calculated as the glucose concentration of the first samples collected (Period 1) minus the glucose concentration of the last samples collected (Period 2), and expressed as per centimeter perfused bowel. (B) Concentration-dependence of inhibition of glucose absorption by GIP in wild-type mice. Data are shown as means with SEM ($n = 6$ for each group, $P < 0.05$ by ANOVA).

2.7. Analysis

The results are given as mean ± standard error (SEM, n = number of mice). Statistical significance was determined using paired and unpaired Student's t-test and analysis of variance (ANOVA). $P < 0.05$ was considered significant.

3. Results

3.1. Perfusion experiment

Inhibition of glucose absorption was calculated by change in glucose concentration in effluent perfusate in wild-type mice (Fig. 1A). Spontaneous inhibition of glucose absorption of 49 ± 44 nmol/cm/15 min is shown in saline-administered controls (Fig. 1B). Inhibition of glucose absorption was enhanced to 67 ± 40, 163 ± 84, and 409 ± 96 nmol/cm/15 min when the amount of intraperitoneally-administered GIP was increased to 12.5, 25, and 50 nmol/kg body weight, respectively.

3.2. Glucose uptake by jejunum in vitro

We investigated glucose uptake by the jejunum *in vitro* using everted jejunal rings. In the presence of 100 nM GIP in the incubation medium, glucose uptake into jejunal rings in wild-type mice was similar to that in the presence of vehicle (control: 4.2 ± 0.9 μmol/g weight; GIP: 3.5 ± 0.9, P = NS; Fig. 2A). Additionally, glucose uptake into jejunal rings in GIPR$^{-/-}$ mice was similar

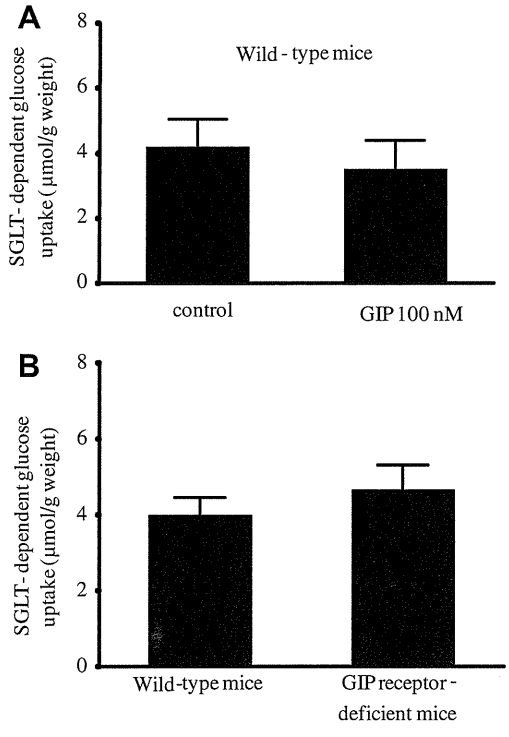

Fig. 2. Glucose uptake in the jejunum. (A) Glucose uptake in the jejunum in wild-type mice in the absence and in the presence of 100 nM GIP. (B) Glucose uptake in the jejunum in wild-type and GIPR$^{-/-}$ mice. SGLT-dependent glucose uptake was determined as the glucose uptake in the absence of 1 mM phlorizin minus the glucose uptake in the presence of 1 mM phlorizin. Data are shown as means with SEM (n = 8 for each group).

to that in wild-type mice (wild-type mice: 4.0 ± 0.5 μmol/g weight; GIPR$^{-/-}$ mice 4.6 ± 0.7, P = NS; Fig. 2B).

3.3. Small intestinal transit after intraperitoneal administration of GIP

Intestinal transit rate was measured by the length of small intestine traversed by the charcoal suspension. In wild-type mice, the intestinal transit rate in GIP-administered mice was significantly less than that in saline-administered control (45 ± 8% vs. 68 ± 4%, $P < 0.01$; Fig. 3A). On the other hand, in GIPR$^{-/-}$ mice, the intestinal transit rate was similar to that in saline-administered control and GIP-administered mice (65 ± 3% vs. 63 ± 4%; Fig. 3B).

3.4. Perfusion and intestinal transit in GLP-1 receptor-deficient mice

To determine whether GIP affects intestinal glucose absorption through GLP-1 signaling, inhibition of glucose absorption by GIP was measured in GLP-1R$^{-/-}$ mice. Inhibition of glucose absorption in GLP-1R$^{-/-}$ mice was 44 ± 100 nmol/cm/15 min in saline-administered control mice and 426 ± 104 nmol/cm/15 min in GIP-administered mice (50 nmol/kg body weight, $P < 0.05$, Fig. 3C). Thus, GIP significantly inhibited glucose absorption in GLP-1R$^{-/-}$ mice.

The intestinal transit rate was also evaluated in GLP-1R$^{-/-}$ mice, and was 59 ± 13% in saline-administered control and 42 ± 7% in GIP-administered mice, respectively. Thus, GIP significantly inhibited the intestinal transit rate in GLP-1R$^{-/-}$ mice ($P < 0.01$, Fig. 3D). Consequently, the genetic disruption of GLP-1 receptor did not affect GIP action on intestinal glucose absorption and intestinal transit.

3.5. Involvement of SST in the action of GIP

To determine whether the inhibitory effect of GIP on intestinal transit is due to release of SST, a somatostatin receptor antagonist, CSS (1 μg/kg body weight), was intraperitoneally administered 10 min prior to GIP administration in wild-type mice (Fig. 4A). In the presence of CSS, the intestinal transit rate in GIP-administered wild-type mice was significantly higher than that in the absence of CSS (60 ± 3% vs. 45 ± 8%; $P < 0.01$). Accordingly, CSS reduced the inhibitory effect of GIP on intestinal transit. Moreover, intraperitoneally-administered SST itself significantly inhibited the intestinal transit rate in wild-type mice compared to control (SST: 37 ± 5% vs. control: 68 ± 4%, $P \leqslant 0.01$).

In a perfusion experiment, to confirm that the inhibitory effect of GIP on intestinal glucose absorption is attributable to release of SST, CSS (1 μg/kg body weight) was intraperitoneally administered 10 min prior to GIP administration in wild-type mice (Fig. 4B). In

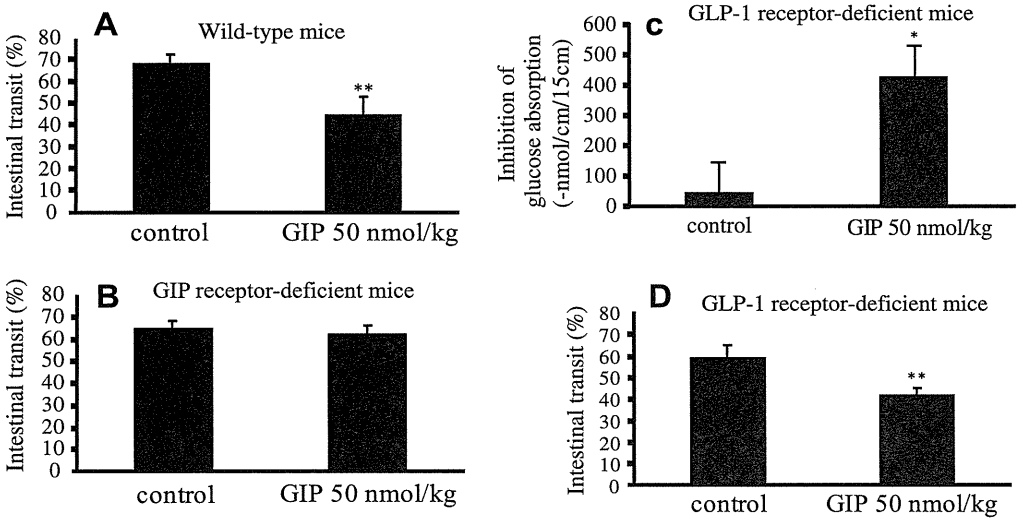

Fig. 3. Intestinal transit after oral administration of non-absorbed marker (10% charcoal suspension in 5% gum Arabic) in wild-type (A) and GIPR$^{-/-}$ (B) mice. Twenty minutes after administration of non-absorbed marker by gavage, the animals were killed and the entire gastrointestinal transit tract was removed. GIP (50 nmol/kg body weight) or saline was administered intraperitoneally 15 min prior to the administration of non-absorbed marker. Data are shown as means with SEM (n = 6 for each group). Statistical significance was determined using Student's t-test. $^{**}P < 0.01$ compared with control. (C) Inhibition of glucose absorption in GLP-1R$^{-/-}$ mice with or without intraperitoneal GIP administration as indicated in the legends of Fig 1. (D) Intestinal transit after oral administration of non-absorbed marker in GLP-1R$^{-/-}$ mice with or without intraperitoneal GIP administration as indicated in the legends of Fig 3A. Data are shown as means with SEM (n = 6 for each group). Statistical significance was determined using Student's t-test. $^{*}P < 0.05$ compared with control.

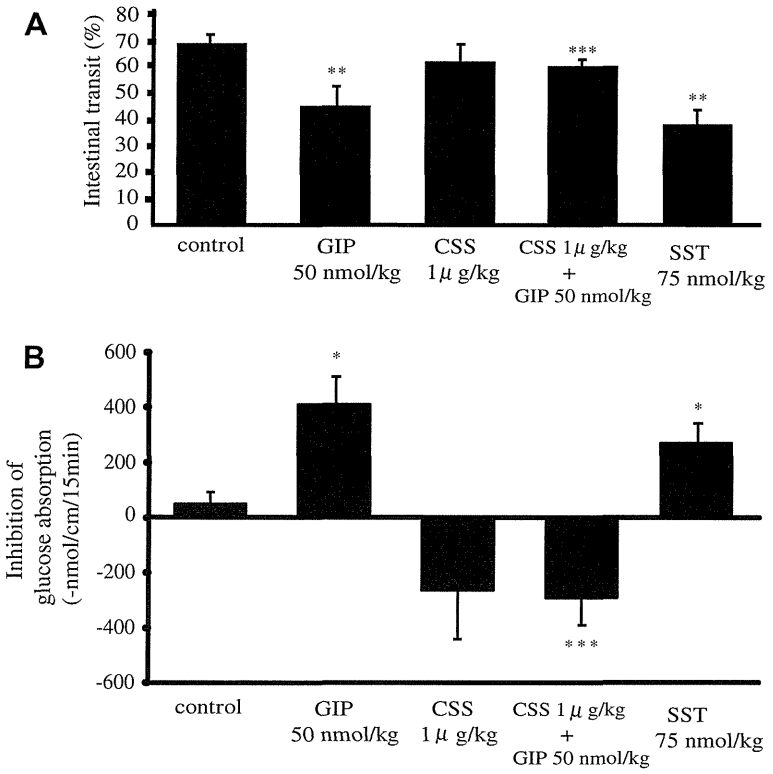

Fig. 4. (A) Intestinal transit after oral administration of non-absorbed marker in wild-type mice with or without pretreatment of CSS. The rate of transit was determined as indicated in the legend of Fig 3A. GIP or SST or saline was administered intraperitoneally 15 min prior to the administration of non-absorbed marker. CSS or saline was intraperitoneally administered 10 min prior to GIP administration. Data are shown as means with SEM ($n = 6$ for each group). Statistical significance was determined using Student's t-test. $^{**}P < 0.01$ compared with control. $^{***}P < 0.01$ compared with GIP alone administered mice. (B) Inhibition of glucose absorption by GIP in wild-type mice with or without pretreatment of CSS, and inhibition of glucose absorption by SST. CSS or saline was intraperitoneally administered 10 min prior to GIP administration. Data are shown as means with SEM ($n = 6$ for each group). Statistical significance was determined using Student's t-test. $^{*}P < 0.05$ compared with control. $^{***}P < 0.01$ compared with GIP alone administered mice.

the presence of CSS, the inhibition of glucose absorption in GIP-administered wild-type mice was significantly lower than that in the absence of CSS (410 ± 96 nmol/cm/15 min vs. −290 ± 99 nmol/cm/15 min; $P < 0.01$). Accordingly, CSS reduced the inhibitory effect of GIP on intestinal glucose absorption. Furthermore, inhibition of glucose absorption in wild-type mice was 49 ± 44 nmol/cm/15 min in saline-administered control mice and 278 ± 63 nmol/cm/15 min in SST-administered mice (75 nmol/kg body weight, $P < 0.05$).

In an experiment of glucose uptake in everted jejunal ring, 100 nM SST did not alter glucose uptake compared to control (control: 4.2 ± 0.9 μmol/g weight; SST: 4.2 ± 0.4, $n = 8$; P = NS).

3.6. Measurement of plasma GIP and SST levels

The plasma levels of total GIP and SST in mice were significantly enhanced 20 min after the intraperitoneal GIP-administration at a dosage of 50 nmol/kg body weight compared to the respective basal levels (GIP: 58 ± 5 pg/ml vs. 3400 ± 257 pg/ml, $n = 8$; $P < 0.01$; SST: 9.9 ± 0.5 ng/ml vs.11.9 ± 0.3 ng/ml, $n = 8$; $P < 0.05$).

4. Discussion

We investigated the inhibitory effect of exogenous GIP on glucose absorption in small intestine. GIP has been known as an important insulinotropic hormone released from duodenal K cells. However, there have been few reports on the effects of GIP on intestinal glucose absorption. In this study, GIP was found to inhibit glucose absorption in a concentration-dependent manner by the perfusion method.

Glucose absorption includes two steps in enterocytes, permeation through brush-border membrane and subsequently through basolateral membrane. Glucose and galactose cross the brush-border membrane by means of SGLT-1, which is a rate-limiting step of glucose absorption [10]. Recent *in vitro* study by Singh et al. found that exogenous GIP stimulates SGLT-dependent glucose absorption by using an Ussing chamber experiment [11]. In the experiment, intestine was fixed between two chambers, and short-circuit-current representing SGLT activity was measured. However, in our experiments using everted jejunal rings, which is another method to measure SGLT-dependent glucose absorption *in vitro*, the lack of effect of exogenous GIP on SGLT-dependent glucose uptake was shown, and genetic disruption of the GIP receptor was found not to affect SGLT-dependent glucose absorption. The reason why our results and theirs are different is unknown, but may be attributable to difference in method.

It is generally accepted that there is a positive relationship between intestinal motility and absorption [4,5]. It has been shown that increased intestinal motility, besides enhancing the functional surface area, facilitates diffusion of glucose to the transporters of the brush-border membrane by altering the unstirred water layer [12,13]. We investigated the effect of GIP on motility of small intestine by evaluating intestinal transit. In this study, GIP was found to inhibit intestinal transit compared to control in wild-type but not in $GIPR^{-/-}$ mice. Thus, the inhibitory effect of GIP on glucose absorption may be attributable, in part, to inhibition of intestinal motility.

GLP-1, another incretin hormone, is secreted from L cells found predominantly in ileal mucosa, and is known to be part of the "ileal brake" that acts as an inhibitor of upper gastrointestinal motility

[14]. In this study, GIP was found to inhibit intestinal transit in GLP-1R$^{-/-}$ mice as well as in wild-type mice, indicating that the inhibitory action of GIP on gastrointestinal transit is not mediated by GLP-1. Furthermore, glucose absorption was found to be inhibited significantly by GIP in GLP-1R$^{-/-}$ mice as well as in wild-type mice, suggesting that the primary mechanism of the inhibition of intestinal glucose absorption by GIP most likely does not involve the GLP-1-mediated pathway.

Recently, Miki et al. reported that GLP-1 inhibited gut motility while GIP did not [15]. In this study, however, GIP was found to inhibit intestinal transit. The inconsistency could be due to their use of a non-absorbed marker containing a high concentration (as much as 50%) of glucose to evaluate gut motility, whereas we used a non-absorbed marker without glucose. Intraduodenal infusion of hyperosmolar solution was reported to increase duodenal motility, which is mediated by activation of osmoreceptors in duodenum [16]. In our preliminary experiment on small intestinal transit using 10% charcoal suspension in 5% gum Arabic with 50% glucose, the intestinal transit rate was significantly greater than that when using glucose-free solution (88 ± 8% vs. 68 ± 4%, $P < 0.05$, unpublished data). Therefore, intestinal transit might be enhanced by the high concentration of glucose itself in the suspension, which could conceal a GIP-evoked inhibitory effect on intestinal transit. However, limitations of this study must be considered. While GIP was found to inhibit intestinal transit under the conditions of this study, the effect of GIP on intestinal transit may differ among the constituents of the food or nutrient. Further investigations are required.

Regarding the GIP dosage applied in the *in vivo* experiments, low GIP dosage has been used when applied by the route of continuous intravenous administration; GIP (0.25 nmol/kg body weight) was reported to stimulate insulin secretion by intravenous administration in rat [17] and (GIP 4 pmol/kg body weight/min) in human [18]. However, high GIP dosage has been used when applied by the other routes of administration than intravenous administration. Indeed, one group has reported that subcutaneous pre-administration of 100 μg GIP (approximately 800 nmol/kg body weight) lowered glucose excursion in oral glucose tolerance test in mice [15] and another group has reported that intraperitoneal administration of [D-Ala^2]GIP (48 nmol/kg body weight/day), a DPP4-resistant analogue, lowered glucose excursion in intraperitoneal glucose tolerance test in mice [19]. In this study, we applied GIP intraperitoneally at a dosage of 50 nmol/kg body weight to demonstrate the pharmacological effects of GIP on intestinal transit and glucose absorption, which dosage is comparable to those used in the latter reports.

Regarding the mechanism of inhibition of intestinal transit by GIP, SST secretion has been reported to be stimulated by GIP [20–22] and to prolong intestinal transit [23,24]. The SST receptor has five isoforms (sst1-5) and all five receptors have been shown to be expressed in gastrointestinal tract, with high levels of sst2 receptor in intestine [25]. The sst2 receptors in intestine have been shown not to be expressed on enterocytes or muscle cells, but on myenteric and submucosal plexuses and on neuroendocrine cells in epithelium [26] and also on interstitial cells of Cajal in deep muscular plexus [27]. Thus, the mechanisms by which exogenous GIP inhibits intestinal motility through two SST-mediated pathways may be as follows. In the first, exogenous GIP binds to the GIP receptors on the cell surface membrane in SST-containing enteric neurons and/or in mucosal endocrine cells of D cells in gastrointestinal tract and/or in pancreatic islets, resulting in the release of SST. Subsequently, the released SST acts as a neurotransmitter and binds to sst2 receptors expressed on other neurons in myenteric plexus, parts of which nerve fibers are distributed to muscular cells, permitting inhibition of intestinal motility. In this pathway, the local SST concentration in interneural synaptic space may be increased prominently. In an alternate pathway, SST secreted from D cells flows into systemic circulation through submucosal vessels to reach the neurons in myenteric plexus. Indeed, in this study, intraperitoneally-administered GIP induced a small but significant increase in plasma SST levels, suggesting involvement of the latter pathway.

In our experiment of intestinal perfusion, GIP was found to inhibit intestinal glucose absorption primarily by reducing intestinal motility. On the other hand, the tissue of everted intestinal ring is set inside-out and distended far from the physiological condition, and thus incapable of reflecting general intestinal motility. Thus, the lack of GIP action on glucose uptake in the tissues of everted intestinal ring in this study may be expected.

Several studies have found that the inhibitory effect of SST on intestinal glucose absorption may be attributable to either the effect of SST on the splanchnic hemodynamics [28] or a direct effect of SST on enterocytes [29]. However, consistent with this study, another study has found that SST delays intestinal glucose absorption by its inhibitory effect on intestinal motility [24]. SST exerts its inhibitory effect on intestinal glucose absorption by several mechanisms; our results indicate that the inhibitory effect of SST is mediated, at least in part, by alteration of intestinal motility.

In this study, the somatostatin receptor antagonist CSS was found to reduce the inhibitory effect of GIP on intestinal transit, suggesting that GIP stimulates SST release. In addition, we show that SST itself inhibits intestinal transit and glucose absorption in perfused intestine. Consistently, a recent study has reported that SST inhibits intestinal glucose absorption [29]. Considered together with previous reports, we conclude that exogenous GIP inhibits intestinal transit and glucose absorption indirectly through a somatostatin-mediated pathway.

One of the physiological roles of GIP is known to be facilitation of nutrient uptake into adipose tissue and bone. In this study, exogenous GIP was found to inhibit intestinal glucose absorption by reducing intestinal motility. Since this observation was obtained by the action of a supraphysiological level of plasma GIP, it is unclear whether or not the action is associated with already known physiological actions of GIP. In the point of delay of intestinal carbohydrate absorption, however, the biological action of GIP found in this study appears to be similar to that of medical medicine α-glucosidase inhibitor, which does not influence the regulation of energy accumulation in adipose tissue or bone.

Acknowledgments

This study was supported by Scientific Research Grants and a Grant for Leading Project for Biosimulation from the Ministry of Education, Culture, Sports, Science, and Technology of Japan, a grant from CREST of Japan Science and Technology Cooperation, and a grant from the Ministry of Health, Labor, and Welfare, Japan, and also by Kyoto University Global COE Program "Center for Frontier Medicine". The authors are grateful to Dr. Daniel J. Drucker for kindly providing GLP-1R$^{-/-}$ mice.

References

[1] Y. Seino, M. Fukushima, D. Yabe, GIP and GLP-1, the two incretin hormones: similarities and differences, J. Diabetes Invest. 1 (2010) 8–23.
[2] K. Miyawaki, Y. Yamada, H. Yano H, et al., Glucose intolerance caused by a defect in the entero-insular axis: a study in gastric inhibitory polypeptide receptor knockout mice, Proc. Natl. Acad. Sci. USA 96 (1999) 14843–14847.
[3] T.B. Usdin, E. Mezey, D.C. Button, et al., Gastric inhibitory polypeptide receptor, a member of the secretin-vasoactive intestinal peptide receptor family, is widely distributed in peripheral organs and the brain, Endocrinology 133 (1993) 2861–2870.
[4] M. Sababi, U.H. Bengtsson, Enhanced intestinal motility influences absorption in anaesthetized rat, Acta Physiol. Scand. 172 (2001) 115–122.
[5] A.J. Smout, Small intestinal motility, Curr. Opin. Gastroenterol. 20 (2004) 77–81.

[6] L.A. Scrocchi, T.J. Brown, N. MaClusky, et al., Glucose intolerance but normal satiety in mice with a null mutation in the glucagon-like peptide 1 receptor gene, Nat. Med. 2 (1996) 1254–1258.
[7] R. Athman, A. Tsocas, O. Presset, et al., In vivo absorption of water and electrolytes in mouse intestin, Application to villin$^{-/-}$ mice, Am. J. Physiol. Gastrointest. Liver Physiol. 282 (2002) G634–639.
[8] K. Tsukiyama, Y. Yamada, K. Miyawaki, et al., Gastric inhibitory polypeptide is the major insulinotropic factor in K(ATP) null mice, Eur. J. Endocrinol. 151 (2004) 407–412.
[9] K. Yamada, M. Hosokawa, S. Fujimoto, et al., The spontaneously diabetic Torii rat with gastroenteropathy, Diabetes Res. Clin. Pract. 75 (2007) 127–134.
[10] M.A. Hediger, M.J. Coady, T.S. Ikeda, et al., Expression cloning and cDNA sequencing of the Na^+/glucose co-transporter, Nature 330 (1987) 379–381.
[11] S.K. Singh, A.C. Bartoo, S. Krishnan, et al., Glucose-dependent insulinotropic polypeptide (GIP) stimulates transepithelial glucose transport, Obesity 16 (2008) 2412–2416.
[12] F.A. Wilson, J.M. Dietschy, The intestinal unstirred layer: its surface area and effect on active transport kinetics, Biochim. Biophys. Acta 363 (1974) 112–126.
[13] D.V. Rayner, The relationships between glucose absorption and insulin secretion and the migrating myoelectric complex in the pig, Exp. Physiol. 76 (1991) 67–76.
[14] A. Wettergren, B. Schjoldager, P.E. Mortensen, et al., Truncated GLP-1 (proglucagon 78–107-amido) inhibits gastric and pancreatic functions in man, Dig. Dis. Sci. 38 (1993) 665–673.
[15] T. Miki, K. Minami, H. Shinozaki, et al., Distinct effects of glucose-dependent insulinotropic polypeptide and glucagon-like peptide-1 on insulin secretion and gut motility, Diabetes 54 (2005) 1956–1963.
[16] H.C. Lin, J.D. Elashoff, G.M. Kwok, et al., Stimulation of duodenal motility by hyperosmolar mannitol depends on local osmoreceptor control, Am. J. Physiol. 266 (1994) G940–943.
[17] E.L. Mazzaferri, L. Ciofalo, L.A. Waters, et al., Effects of gastric inhibitory polypeptide on leucine- and arginine-stimulated insulin release, Am. J. Physiol. 245 (1983) E114–E120.
[18] T. Vilsbøll, T. Krarup, S. Madsbad, et al., Defective amplification of the late phase insulin response to glucose by GIP in obese Type II diabetic patients, Diabetologia 45 (2002) 1111–1119.
[19] B.J. Lamont, D.J. Drucker, Differential antidiabetic efficacy of incretin agonists versus DPP-4 inhibition in high fat fed mice, Diabetes 57 (2008) 190–198.
[20] J. Szecówka, V. Grill, E. Sandberg, et al., Effect of GIP on the secretion of insulin and somatostatin and the accumulation of cyclic AMP in vitro in the rat, Acta Endocrinol. (Copenh) 99 (1982) 416–421.
[21] L. Hansen, J.J. Holst, The effects of duodenal peptides on glucagon-like peptide-1 secretion from the ileum. A duodeno–ileal loop?, Regul Pept. 110 (2002) 39–45.
[22] J.J. Holst, S.L. Jensen, S. Knuhtsen, et al., Effect of vagus, gastric inhibitory polypeptide, and HCl on gastrin and somatostatin release from perfused pig antrum, Am. J. Physiol. 244 (1983) G515–522.
[23] G.J. Krejs, Effect of somatostatin and absorption and atropine infusion on intestinal transit tine and fructose absorption in the perfused human jejunum, Diabetes 33 (1984) 548–551.
[24] C. Johansson, O. Wisén, S. Efendić, et al., Effects of somatostatin on gastrointestinal propagation and absorption of oral glucose in man, Digestion 22 (1981) 126–137.
[25] K. Krempels, B. Hunyady, A.M. O'Carroll, et al., Distribution of somatostatin receptor messenger RNAs in the rat gastrointestinal tract, Gastroenterology 112 (1997) 1948–1960.
[26] M. Gugger, B. Waser, A. Kappeler, et al., Cellular detection of sst2A receptors in human gastrointestinal tissue, Gut 53 (2004) 1431–1436.
[27] C. Sternini, H. Wong, S.V. Wu, et al., Somatostatin 2A receptor is expressed by enteric neurons, and by interstitial cells of Cajal and enterochromaffin-like cells of the gastrointestinal tract, J. Comp. Neurol. 386 (1997) 396–408.
[28] J. Wahren, Influence of somatostatin on carbohydrate disposal and absorption in diabetes mellitus, Lancet 2 (1976) 1213–1216.
[29] F. Féry, L. Tappy, P. Schneiter, et al., Effect of somatostatin on duodenal glucose absorption in man, J. Clin. Endocrinol. Metab. 90 (2005) 4163–4169.

Molecular Genetics and Metabolism 102 (2011) 453–460

Contents lists available at ScienceDirect

Molecular Genetics and Metabolism

journal homepage: www.elsevier.com/locate/ymgme

GCKR mutations in Japanese families with clustered type 2 diabetes

Daisuke Tanaka [a], Kazuaki Nagashima [a], Mayumi Sasaki [a], Chizumi Yamada [a], Shogo Funakoshi [a], Kimiyo Akitomo [a], Katsunobu Takenaka [b], Kouji Harada [c], Akio Koizumi [c], Nobuya Inagaki [a,*]

[a] *Department of Diabetes and Clinical Nutrition, Graduate School of Medicine, Kyoto University, Kyoto, Japan*
[b] *Takayama Red Cross Hospital, Gifu, Japan*
[c] *Department of Health and Environmental Sciences, Graduate School of Medicine, Kyoto University, Kyoto, Japan*

ARTICLE INFO

Article history:
Received 15 December 2010
Accepted 15 December 2010
Available online 21 December 2010

Keywords:
Genetic susceptibility
Linkage analysis
MODY
HNF1A
GCKR

ABSTRACT

Objective: The aim was to investigate the genetic background of familial clustering of type 2 diabetes.
Subjects and methods: We recruited Japanese families with a 3-generation history of diabetes. Genome-wide linkage analysis was performed assuming an autosomal dominant model. Genes in the linkage region were computationally prioritized using Endeavour. We sequenced the candidate genes, and the frequencies of detected nucleotide changes were then examined in normoglycemic controls.
Results: To exclude known genetic factors, we sequenced 6 maturity onset diabetes of the young (MODY) genes in 10 familial cases. Because we detected a MODY3 mutation *HNF1A* R583G in one case, we excluded this case from further investigation. Linkage analysis revealed a significant linkage region on 2p25-22 (LOD score = 3.47) for 4 families. The 23.6-Mb linkage region contained 106 genes. Those genes were scored by computational prioritization. Eleven genes, i.e., top 10% of 106 genes, were selected and considered primary candidates. Considering their functions, we eliminated 3 well characterized genes and finally sequenced 8 genes. *GCKR* ranked highly in the computational prioritization. Mutations (minor allele frequency less than 1%) in exons and the promoter of *GCKR* were found in index cases of the families (3 of 18 alleles) more frequently than in controls (0 of 36 alleles, P = 0.033). In one pedigree with 9 affected members, the mutation *GCKR* g.6859C>G was concordant with affection status. No mutation in other 7 genes that ranked highly in the prioritization was concordant with affection status in families.
Conclusions: We propose that *GCKR* is a susceptibility gene in Japanese families with clustered diabetes. The family based approach seems to be complementary with a large population study.

1. Introduction

The national survey in 2007 reported that 8.9 million people suffer from diabetes in Japan [1]. Most of these have type 2 diabetes, and the number of such patients has increased continuously. Both genetic and environmental factors play important roles in the pathogenesis of type 2 diabetes [2].

To elucidate the genetic factors underlying the pathogenesis of type 2 diabetes in the Japanese population, several genome-wide linkage analyses in Japanese sib-pairs have been performed [3–5]. Linkage to 11p13–p12 is consistently implicated in these studies [5]. Recent successes with genome-wide association analyses in the Japanese population have revealed a susceptibility variant in *KCNQ1* located at 11p15.5 [6,7], a locus not far from the region suggested in linkage analyses. The association of susceptibility loci including *TCF7L2*, *CDKAL1*, *CDKN2A/B*, *IGF2BP2*, *SLC30A8*, and *HHEX* with diabetes has been established in Caucasian populations and replicated in the Japanese population [8]. However, the loci identified in association studies have uniformly small effect sizes, and can explain only a small portion of the genetic background of diabetes in the Japanese population. Approaches other than sib-pair linkage analyses and association analyses may therefore be required to elucidate a greater aspect of the genetic background of type 2 diabetes.

In the present study, we used a family-based approach, because high degrees of familial clustering can raise the relative risk and provide better insight to novel loci of larger effect size [9]. Familial clustering of diabetes is well known, the typical example being MODY [10]. On the other hand, in most families in Japan, familial clustering cannot be attributed to mutations of the 6 known MODY genes [10], and genetic predisposition in such families has not been ascertained.

We recruited families having a 3-generation history of diabetes and performed genome-wide linkage analysis. We selected candidate genes in the linked chromosomal region and searched for rare and

Abbreviations: GAD, glutamic acid decarboxylase; GCKR, glucokinase regulator; HLOD, heterogeneity logarithm of the odds; HNF4α, Hepatocyte Nuclear Factor 4α; LOD, logarithm of the odds; MAF, minor allele frequency; MODY, maturity onset diabetes of the young; RFLP, restriction fragment length polymorphism; SNP, single nucleotide polymorphism.

* Corresponding author. Department of Diabetes and Clinical Nutrition, Graduate School of Medicine, Kyoto University, 54 Shogoin-Kawahara-cho, Sakyo-ku, Kyoto, 606-8507, Japan. Fax: +81 75 771 6601.
E-mail address: inagaki@metab.kuhp.kyoto-u.ac.jp (N. Inagaki).

1096-7192/$ – see front matter © 2010 Elsevier Inc. All rights reserved.
doi:10.1016/j.ymgme.2010.12.009

common nucleotide changes in the genes in familial cases and unaffected controls.

2. Material and methods

2.1. Families and additional index cases

We recruited patients from collaborating hospitals in Japan who had diabetes with a 3-generation family history, which is suggestive of autosomal dominant mode of inheritance [11]. If ≥2 family members with diabetes were alive and donated DNA, the families were regarded as suitable subjects for the present study. Families including members with positive GAD (glutamic acid decarboxylase) antibody were excluded from the study. Four families met these criteria and were included in the linkage analysis (Fig. 1). Affected status of the participants was determined in two ways. First, if participants had been diagnosed with diabetes and treated with oral hypoglycemic agents or insulin injection, they were regarded as affected. Second, if participants had not been treated with oral hypoglycemic agents or insulin injection, they underwent HbA1c (Hemoglobin A_{1c}) measurement for screening of impaired glucose tolerance. The value for HbA1c is estimated as an NGSP (US National Glycohemoglobin Standardization Program) equivalent value (%) calculated by the formula HbA1c (%) = HbA1c (JDS, Japanese Diabetes Society) (%) + 0.4%, considering the relational expression of HbA1c (JDS)(%) measured by the previous Japanese standard substance and measurement methods and HbA1c (NGSP) [12]. If their HbA1c levels were ≥6.0%, they were also regarded as affected. HbA1c ≥6.0% is the level defined as possible diabetes mellitus in the 2007 survey of the Ministry of Labor, Health and Welfare of Japan [1]. In addition to these subjects, 6 index cases from other families with a 3-generation history of diabetes were included in the study (Supplementary Fig. 1). In these families, although we confirmed the affected status of some of the family members, DNA samples were available only for the index cases but not for other family members. Together with the 4 index cases from the families included in the linkage analysis, a total of 10 unrelated cases with a 3-generation history of diabetes were available for DNA sequencing. The clinical features of family members and additional index cases are shown in Table 1.

2.2. Normoglycemic controls

An annual medical check-up program was performed in Nyukawa district of Takayama City, Japan. Nine-hundred ninety local residents (430 men, 560 women) were recruited in the program and consented to donate their DNA. From 2002 to 2007, participants underwent physical examination and blood tests including fasting plasma glucose and HbA1c every year. We selected normoglycemic controls from the

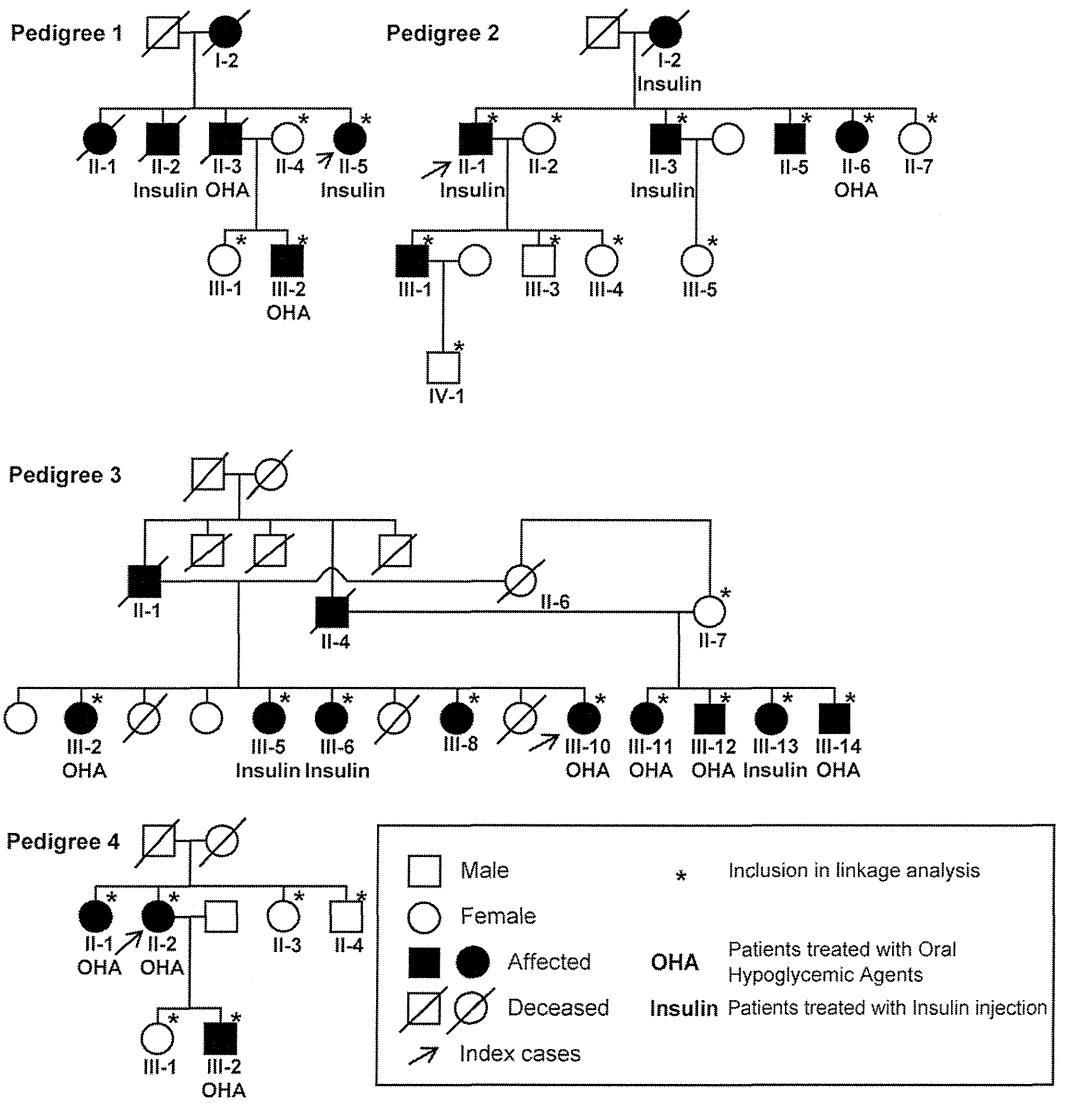

Fig. 1. Four pedigrees with familial aggregated diabetes mellitus.

Table 1
Characteristics of family members and additional index cases.

	ID	Current age	Sex	BMI	HbA1c (%)	Age when diagnosed (diagnosis)	Current therapy
Pedigree 1	II-4	70	F	16.2	5.0		
	II-5	71	F	22.5	10.6	60 (DM)	Insulin 66 U/d
	III-1	40	F	21.9	5.4		
	III-2	37	M	26.0	6.9	20 (DM)	Insulin
Pedigree 2	II-1	79	M	19.2	7.5	50 (DM)	Insulin 25 U/d
	II-2	77	F	18.6	5.6		
	II-3	76	M	17.9	7.2	45 (DM)	Insulin
	II-5	74	M	18.2	6.0	64 (IGT)	Diet
	II-6	71	F	18.4	6.6	N/A (DM)	Oral drug
	II-7	68	F	19.9	5.9		
	III-1	53	M	24.2	6.0	53 (IGT)	Diet
	III-3	51	M	20.4	5.6		
	III-4	47	F	19.3	5.2		
	III-5	46	F	19.6	4.9		
	IV-1	23	M	19.9	5.6		
Pedigree 3	II-7	92	F	22.3	5.9		
	III-2	77	F	23.9	9.3	30 (DM)	Oral drug
	III-5	72	F	22.0	8.1	60 (DM)	Insulin 16 U/d
	III-6	69	F	19.8	8.0	65 (DM)	Insulin 16 U/d
	III-8	66	F	19.1	6.5	64 (IGT)	Diet
	III-10	59	F	19.3	10.2	57 (DM)	Oral drug
	III-11	67	F	20.4	6.9	62 (DM)	Oral drug
	III-12	66	M	21.1	N/A	57 (DM)	Oral drug
	III-13	64	F	20.0	6.6	25 (DM)	Insulin
	III-14	62	M	20.2	10.3	50 (DM)	Oral drug
Pedigree 4	II-1	76	F	28.2	6.7	60 (DM)	Oral drug
	II-2	73	F	25.1	6.4	50 (DM)	Oral drug
	II-3	67	F	19.0	5.5		
	II-4	64	M	N/A	5.4		
	III-1	52	F	20.4	5.3		
	III-2	50	M	20.8	6.2	35 (DM)	Oral drug
Additional index cases	1	57	M	25.7	7.1	30 (DM)	Oral drug
	2	47	F	22.9	10.0	36 (DM)	Insulin 20 U/d
	3	68	F	19.7	7.1	45 (DM)	Insulin 19 U/d
	4	60	F	24.7	10.4	40 (DM)	Insulin 51 U/d
	5	60	F	28.0	9.7	50 (DM)	Insulin 8 U/d
	6	54	F	34.5	9.1	40 (DM)	Insulin

BMI: body mass index, DM: diabetes mellitus, IGT: impaired glucose tolerance.

participants in the cohort. Subjects defined as normoglycemic controls had the following characteristics: HbA1c <6.0% and fasting plasma glucose <5.5 mmol/l during 5-year follow-up span, and age ≥55. The number of subjects that satisfied the definition was 206 (81 men, 125 women).

2.3. Genotyping family members

Genomic DNA was extracted from blood samples with a QIAamp DNA Blood Mini Kit (Qiagen Inc). PCR amplification from genomic DNA was performed with fluorescence-labeled (6-FAM, HEX, NED) and tailed primers. PCR primers to analyze microsatellite markers comprised an approximately 10 cM human index map (ABI Prism Linkage Mapping Set Version 2.5: 382 markers for 22 autosomes), and other microsatellite fine markers were designed according to information from the UniSTS map. PCR reactions were carried out in 7.5 μl with 50 ng genomic DNA, using AmpliTaq Gold DNA Polymerase (Applied Biosystems) in a 2-step amplification program. DNA fragments were analyzed on an Applied Biosystems 3130 Genetic Analyzer. Genotyping errors and inconsistent relationships were checked with the use of GENEHUNTER (version 2.1) software [13]. If the results of genotyping were missed or ambiguous, we treated them as an unknown genotype in the linkage analysis. The rate of genotyping failure was 0.057% (7/11842).

2.4. Linkage and haplotype analyses

Both affected and unaffected family members were included in the linkage analysis. Participants with HbA1c level <6.0% were considered unaffected if the age was ≥55 and unknown if the age was <55, considering the assumed age-dependent penetrance of diabetes. The purpose of including members assigned as unknown was to increase the accuracy of haplotype estimation in affected members, although inclusion did not increase the statistical power. Multipoint parametric analyses for autosomes were run using GENEHUNTER assuming an autosomal dominant model [13]. Because locus heterogeneity could be associated with diabetes, LOD (log of the odds) score and HLOD (heterogeneity LOD) score were calculated. The disease allele frequency was set at 0.00001 and a phenocopy frequency of 0.00001 was assumed. Population allele frequencies for each microsatellite marker were assigned equal portions for individual alleles. We used a 2-stage design: first, all chromosomal regions were screened by genotyping at an approximately 10 cM density (screening), and the regions where LOD scores were highest were considered potentially interesting. Second, these regions were further finely mapped at approximately 1- to 2-cM densities (fine mapping). Regions where LOD scores were above 3.3, a level corresponding to genome-wide significance [9], were considered linkage regions. Haplotypes were constructed with the GENEHUNTER program.

2.5. Prioritization of candidate genes

The 23.6-Mb linkage region on chromosome 2p25-22 contained 106 genes annotated in Ensemble genome browser (http://www.ensembl.org). The genes were computationally prioritized using Endeavour (http://www.esat.kuleuven.be/endeavour/) [14]. We selected 6 MODY genes (*HNF4A*, *GCK*, *HNF1A*, *PDX1*, *HNF1B*, and *NEUROD1*) as training genes because a dominant mode of inheritance